

**SYSTEM PARAMETER ADAPTATION BASED ON IMAGE  
METRICS FOR AUTOMATIC TARGET DETECTION**

**A THESIS SUBMITTED TO  
THE GRADUATE SCHOOL OF NATURAL AND APPLIED SCIENCES  
OF  
THE MIDDLE EAST TECHNICAL UNIVERSITY**

**BY**

**KENAN KÜREKLİ**

**IN PARTIAL FULLFILMENT OF THE REQUIREMENTS FOR THE DEGREE OF  
MASTER OF SCIENCE  
IN  
THE DEPARTMENT OF ELECTRICAL AND ELECTRONICS ENGINEERING**

**APRIL-2004**

Approval of the Graduate School of Natural and Applied Sciences.

---

Prof. Dr. Canan ÖZGEN  
Director

I certify that this thesis satisfies all the requirements as a thesis for the degree of Master of Science.

---

Prof. Dr. Mübeccel DEMİREKLER  
Chairman of the Department

This is to certify that we have read this thesis and that in our opinion it is fully adequate, in scope and quality, as a thesis for the degree of Master of Science.

---

Assoc. Prof. Dr. Gözde Bozdağı AKAR  
Supervisor

Examining Committee Members

Prof. Dr. Mübeccel DEMİREKLER \_\_\_\_\_

Prof. Dr. Mete SEVERCAN \_\_\_\_\_

Assoc. Prof. Dr. Gözde Bozdağı AKAR \_\_\_\_\_

Assoc. Prof. Dr. Yasemin Yardımcı ÇETİN \_\_\_\_\_

Assoc. Prof. Dr. Aydın ALATAN \_\_\_\_\_

## **ABSTRACT**

# **SYSTEM PARAMETER ADAPTATION BASED ON IMAGE METRICS FOR AUTOMATIC TARGET DETECTION**

**KÜREKLİ, Kenan**

**M.S., Department of Electrical and Electronics Engineering**

**Supervisor: Assoc. Prof. Dr. Gözde Bozdağı AKAR**

**April 2004, 88 pages**

Automatic object detection is a challenging field which has been evolving over decades. The application areas span many domains such as robotics inspection, medical imaging, military targeting, and reconnaissance. Some of the most concentrated efforts in automatic object detection have been in the military domain, where most of the problems deal with automatic target detection and scene analysis in the outdoors using a variety of sensors.

One of the critical problems in Automatic Target Detection (ATD) systems is multi-scenario adaptation. Most of the ATD systems developed until today perform unpredictably i.e. perform well in certain scenarios, and poorly in others. Unless ATD systems can be made adaptable, their utility in battlefield missions remains questionable.

This thesis describes a methodology that adapts parameterized ATD systems with image metrics as the scenario changes so that ATD system can maintain better performance. The methodology uses experimentally obtained performance models, which are functions of image metrics and system parameters, to optimize performance measures of the ATD system. Optimization is achieved by adapting system parameters with incoming image metrics based on performance models as the system works in field. A simple ATD system is also proposed in this work to describe and test the methodology.

Keywords: Automatic Target Detection, Image Metrics, Performance Models, Experimental Design

## **ÖZ**

# **GÖRÜNTÜ ÖLÇÜTLERİ KULLANIMI İLE OTOMATİK HEDEF TESPİT SİSTEMLERİ İÇİN PARAMETRE ADAPTASYONU**

**KÜREKLİ, Kenan**

**Yüksek Lisans, Elektrik ve Elektronik Mühendisliği Bölümü**

**Tez Yöneticisi : Doç. Dr. Gözde Bozdağı AKAR**

**Nisan 2004, 88 sayfa**

Otomatik nesne tespiti son yıllarda üzerinde çalışmaların yoğunlaştığı önemli bir araştırma alanıdır. Uygulamaları kapsamında tıbbi görüntüleme, robot görüşü, keşif ve askeri hedef tespiti bulunan otomatik nesne tespit çalışmalarında askeri alana yoğun önem verilmiştir. Bu alanda, çeşitli algılayıcılardan gelen işaretler üzerinden otomatik hedef tespiti ve sahne analizi yapılmaya çalışılmıştır.

Otomatik hedef tespit çalışmalarında önemli problemlerden biri her senaryoda çalışabilecek sistemler geliştirmek olmuştur. Bugüne kadar geliştirilen sistemlerin büyük kısmı bu konuda yetersiz kalmaktadır ve bu konu çözülene kadar otomatik hedef tespit sistemlerinin savaş alanında kullanımı soru işareti olarak kalacaktır.

Bu tez çalışmasında parametrelî otomatik hedef tespit sistemlerini, deęişen çalışma senaryolarında, görüntü ölçütlerine göre performansı arttıracak şekilde uyumlayan bir metodoloji anlatılmaktadır. Metodoloji, deneysel olarak elde edilmiş, görüntü ölçütleri ve sistem parametrelerinin bir fonksiyonu olan performans modellerini sistem performansını optimize etmek için kullanılmaktadır. Optimizasyon sistem çalışması sırasında, gelen görüntülerden elde edilen ölçütlerin kullanılması ve buna baęlı olarak sistem parametrelerinin deęiştirilmesiyle sağlanmaktadır. Önerilen metodolojinin tanımlanması ve test edilmesi için örnek bir otomatik hedef tespit sistemi geliştirilmiştir.

Anahtar Kelimeler : Otomatik Hedef Tespiti, Görüntü Ölçütleri, Performans Modeli, Deneysel Tasarım

## ACKNOWLEDGEMENTS

I wish to write this page with sufficient time and in my own language. The first one is absolutely my mistake, for the second one I cannot do anything, at least for today. Nevertheless I have to confess that, not as much as when working for the thesis but writing here is attractive.

First of all I have to thank my supervisor Assoc. Prof. Dr. Gözde Bozdağı Akar. In my conditions this work could not be finished with any other supervisor that I know. Evidences are increased to believe that my grandmother's prays for me are useful.

I want to give my thanks to my family and my friends who pay attention all my words patiently and who were with me. In thesis context, my friend Fatih whom I call to take support to give up the thesis on the last day of submission has a privileged position because of the ungiven support. I cannot be writing these words if I had called my grandmother.

And finally I have to write down my gratitude here to my father who let me learn everything important that cannot be learned in schools, silently. Although this gratitude may never be read by him I am happy to write this in a place where never be erased. I know that this work will not have an importance if it does not be a stair for me to make something worthwhile to dedicate to my father.

## TABLE OF CONTENTS

<b>ABSTRACT .....</b>	<b>iii</b>
<b>ÖZ.....</b>	<b>v</b>
<b>ACKNOWLEDGEMENTS.....</b>	<b>vii</b>
<b>TABLE OF CONTENTS.....</b>	<b>viii</b>
<b>LIST OF TABLES .....</b>	<b>x</b>
<b>LIST OF FIGURES .....</b>	<b>xi</b>
<b>LIST OF ABBREVIATIONS.....</b>	<b>xiv</b>

## CHAPTERS

<b>1. INTRODUCTION.....</b>	<b>1</b>
1.1 Problem Definition.....	1
1.2 Scope of the Thesis .....	2
1.3 Outline of the Thesis .....	4
<b>2. ATD ALGORITHMS .....</b>	<b>5</b>
2.1 Introduction.....	5
2.2 Basic ATD Implementation .....	6
2.3 Historical Development of ATD Systems.....	7
2.4 Proposed ATD System.....	9
<b>3. IMAGE METRICS for ATD Systems.....</b>	<b>27</b>
3.1 Introduction.....	27
3.2 Global Image Metrics.....	28
3.3 Region Dependent Image Metrics.....	36
3.4 Target Dependent Metrics.....	39

<b>4. EXPERIMENTAL DESIGN and PERFORMANCE MODELING</b>	
4.1 Introduction .....	43
4.2 Design of Experiments .....	44
4.3 Performance Model Fitting .....	47
<b>5. OPTIMIZATION and TEST RESULTS .....</b>	<b>63</b>
5.1 Introduction .....	63
5.2 Multiobjective Optimization .....	64
5.3 ATD Optimization .....	67
5.4 Test Results .....	69
<b>6. CONCLUSION and FUTURE WORK.....</b>	<b>79</b>
6.1 Summary and Conclusion .....	79
6.2 Future Work .....	80
<b>REFERENCES.....</b>	<b>82</b>
<b>APPENDIX</b>	
<b>A. Model Information .....</b>	<b>85</b>

## LIST OF TABLES

### TABLE

2.1 Thermal Image Sequences .....	14
2.2 Target Area Statistics .....	16
2.3 Target MBR Area Statistics .....	17
2.4 Target Perimeter Statistics .....	18
2.5 Target Aspect Ratio Statistics .....	19
2.6 Target_Area/MBR_Area Ratio Statistics.....	20
2.7 Target Intensity Mean Statistics.....	21
2.8 Target Intensity Standard Deviation Statistics.....	22
2.9 Training Database Statistics.....	23
2.10 Distance Coefficients .....	24
3.1 A Taxonomy of ATD Metrics.....	27
3.2 Global Image Metrics.....	28
3.3 Region Dependent Image Metrics.....	36
3.4 Target Dependent Image Metrics.....	40
4.1 Factors for RS of Probability of Detection (D-Optimal Design) .....	50
4.2 Factors for RS of Probability of Detection (Full Factorial Design).....	53
4.3 Factor Levels for Full Factorial Design .....	53

## LIST OF FIGURES

### FIGURE

1.1 Overall approach. ....	2
2.1 Typical processing steps for an ATD from the sensor to target discrimination... 6	6
2.2 Processing steps for proposed ATD system.....	9
2.3 Image before median filtering.....	10
2.4 Image after median filtering.....	10
2.5 Image before segmentation. ....	12
2.6 Seed points labeled with white color. ....	12
2.7 Segmented Image. ....	13
2.8 Target area values for thermal camera sequences 09-08-07 .....	15
2.9 Target MBR area values for thermal camera sequences 09-08-07 .....	16
2.10 Target perimeter values for thermal camera sequences 09-08-07 .....	17
2.11 Target aspect ratio values for thermal camera sequences 09-08-07 .....	18
2.12 Target_Area/MBR_Area Ratio values for thermal camera sequences 09-08-07 .....	19
2.13 Target mean intensity values for thermal camera sequences 09-08-07 .....	21
2.14 Target intensity std values for thermal camera sequences 09-08-07 .....	22
3.1 Grey-Level std of thermal camera sequence 09-08-07 .....	29
3.2 Grey-Level entropy of thermal camera sequence 09-08-07.....	30
3.3 Grey-Level uniformity (window size 3x3) of thermal camera sequence 09-08-07 .....	31
3.4 Grey-Level uniformity (window size 5x5) of thermal camera sequence 09-08-07 .....	32
3.5 Co-occurrence matrix based uniformity (distance=3) of thermal camera	

sequence 09-08-07 .....	33
3.6 Co-occurrence matrix based uniformity (distance=5) of thermal camera sequence 09-08-07 .....	34
3.7 Edge based information content (threshold=100) of thermal camera sequence 09-08-07 .....	35
3.8 Edge based information content (threshold=130) of thermal camera sequence 09-08-07 .....	36
3.9 Regional std of thermal camera sequence 09-08-07 .....	38
3.10 Regional contrast of thermal camera sequence 09-08-07 .....	39
3.11 Target to Background contrast of thermal camera sequence 09-08-07.....	41
3.12 Target interference ratio of thermal camera sequence 09-08-07 .....	42
4.1 Response surface for $P_D$ with D-optimal experiments .....	51
4.2 Residual values for RS of $P_D$ with D-optimal experiments .....	52
4.3 Response surface for $P_D$ with D-optimal experiments .....	54
4.4 Residual values (1 to 200) for RS of $P_D$ with full factorial experiments .....	55
4.5 Residual values (2001 to 2200) for RS of $P_D$ with full factorial experiments ...	55
4.6 Response surface for SA with full factorial experiments.....	57
4.7 Residual values (1 to 200) for RS of SA with full factorial experiments .....	58
4.8 Residual values (2001 to 2200) for RS of SA with full factorial experiments ..	59
4.9 Response surface for FAR with full factorial experiments .....	61
4.10 Residual values (1 to 14000) for RS of SA with full factorial experiments ....	62
5.1 Mapping from parameter space into objective function space.....	65
5.2 Set of noninferior solutions .....	66
5.3 Sample frame from test sequence 1 .....	70
5.4 Sample frame from test sequence 2 .....	70
5.5 Target dependent metrics of test sequence 1.....	71
5.6 Target dependent metrics of test sequence 2.....	71
5.7 Probability of Detection (Constraint on FAR) for test sequence 1 .....	73
5.8 Probability of Detection (Constraint on FAR) for test sequence 2 .....	73
5.9 FAR for test sequence 1/2 .....	74
5.10 Probability of Detection (Constraint on SA) for test sequence 1 .....	75

5.11 Probability of Detection (Constraint on SA) for test sequence 2.....	75
5.12 Segmentation Accuracy for test sequence 1.....	76
5.13 Segmentation Accuracy for test sequence 2.....	76
5.14 Non-Optimal Probability of Detection (Constraint on FAR) for test sequence 1 .....	77
5.15 Non-Optimal Probability of Detection (Constraint on FAR) for test sequence 2 .....	78

## LIST OF SYMBOLS

ATD	: Automatic Target Detection
DOE	: Design of Experiments
FAR	: False Alarm Rate
MBR	: Minimum Bounding Rectangle
$P_D$	: Probability of Detection
PM	: Performance Metric
RMSE	: Root Mean Square Error
ROI	: Region of Interest
RS	: Response Surface
SA	: Segmentation Accuracy
SRG	: Seeded Region Growing
Std	: Standard Deviation

# CHAPTER 1

## INTRODUCTION

### 1.1 Problem Definition

Automatic object detection is a challenging field that has been evolving over decades. The application areas span many domains such as robotics inspection, medical imaging, military targeting, and reconnaissance. Some of the most concentrated efforts in automatic object detection have been in the military domain, where most of the problems deal with detection of targets and scene analysis in the outdoors using a variety of sensors [1].

Multi-scenario adaptability is by far the most serious and challenging problem in Automatic Target Detection (ATD) technology. ATD adaptation is not just a desirable feature, but also rather a very critical functional requirement. The problem of multi-scenario adaptation was early realized in the ATD technology. It was well understood that algorithms would perform well with whatever assumptions they were based upon, and that they would detect and recognize targets similar to the ones they were trained on. However, it was assumed that the algorithms were flexible enough, to span a wide range of scenarios. This assumption proved to be wrong when ATD systems were tested in field. Real world scenarios, and even terrain boards, showed that there was too much variation in the content, context and quality of the images. However the ATDs were set up to deal with only a small subset of them [2].

One promising aspect of the adaptation problem is that most ATD systems are parameterized. When tests are performed, tuning a number of algorithm parameters improves the ATD performance. This parameter adaptation requires a human expert because it requires intimate knowledge of the ATD algorithms and its parameters (there are typically many critical parameters in a given ATD). As a result, in the literature the ATD adaptation challenge was slightly scoped to automatic adaptation of ATD system parameters [3].

**1.2 Scope of the Thesis**

The concern of this thesis is to give details of a methodology for *adapting the ATD system parameters, based on image metrics and using formal performance prediction models*. The overall approach is highlighted in Figure 1.1.

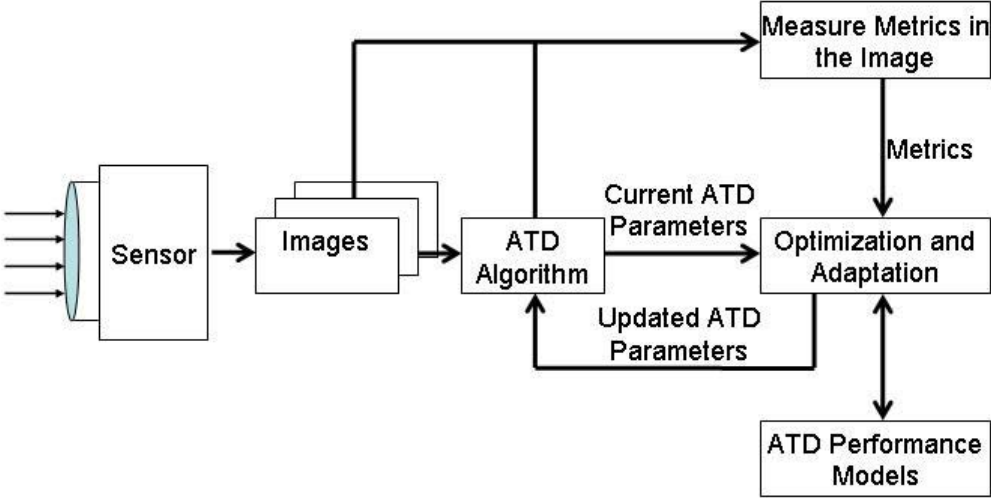


**Figure 1.1** Overall approach.

With this approach, while the ATD system is working in the field, the system measures image metrics from incoming images. Then experimentally obtained (offline) performance models that are functions of the image metrics and the ATD system parameters are used to find the optimal ATD parameters for better system performance.

In other words, given the experimentally obtained ATD performance measure (PM) model,

$$PM = F (M_1, M_2, \dots M_N; P_1, P_2, \dots P_K) \quad (1.1)$$

where  $M_I$  is an image metric and  $P_J$  is a system parameter, and assuming that the image metrics ( $M_I$ ) of the current frame to be processed are known, this approach attempts to find the optimal ATD parameter ( $P_J$ ) values based on the model for better system performance [3].

The success of this approach is highly dependent on the prediction capabilities of the performance models. An ATD performance prediction model, for a performance measure PM (such as Probability of Detection), is a function of one or more image metrics  $M$  (such as Global Uniformity), and one or more ATD system parameters (such as Seed Grow Threshold). With this approach the number and properties of performance measures, image metrics and system parameters are all specifically determined by considering the ATD system configuration.

Once the performance measures, image metrics and parameters are determined, performance models are generated as a result of a number of experiments. Experiments are done to obtain performance measure values for different combinations of the image metric and system parameter values. Performance measure values together with image metric and parameter values are used to fit performance models.

Because the performance models are expressed in mathematical equations, given image metric values, finding the optimum parameters in order to achieve the optimum performance becomes a mathematical optimization problem.

To describe and test the approach given above, a simple ATD system with static parameters is also proposed within this thesis.

### **1.3 Outline of the Thesis**

Chapter 2 gives an overview of ATD systems together with the proposed system. Image metrics that are used for implementing the approach on proposed ATD system are given in Chapter 3. Experimental design of performance models and optimization approach together with test results are explained in Chapter 4 and Chapter 5. Finally, summary, conclusion and future work are given in Chapter 6.

## CHAPTER 2

### ATD ALGORITHMS

#### 2.1. Introduction

One of the key components of present and future defense weapon systems to be used on autonomous defense vehicle missions is the ATD system. The ATD system effectively removes man from the process of target acquisition. This is desirable since the system with a man in the loop is generally slow, unreliable, vulnerable, and may limit the performance of the overall system or mission in real situations [4].

In the military, ATD is used in a number of applications but the most sophisticated example is the fire-and-forget, lock-on-after launch missile. Here, an ATD would recognize the candidate targets in the scene after it has been launched, select the target of choice, track the target during the flight, make final aim point selection, and conduct guidance to the target. In autonomous applications, an image may never be displayed, as in the case of a fire-and-forget missile. Acceptable autonomous operation is still an unattainable goal of ATD in the military. The less ambitious current objective is aided target detection, i.e., the subset of ATD in which a human interacts with the system and makes critical decisions. Research work in this area has been going for the last 35 years and will continue to go based on the shortcomings of the current implementations [1].

The main purpose of this chapter is to give basic information about ATD systems and to propose a simple parameterized ATD system that is going to be used for

describing and testing the adaptation method, which is the objective of this thesis. Basic ATD implementation and historical development of ATD systems are explained in section 2.2 and section 2.3. Proposed ATD system that is used throughout this work is described in section 2.4 of this chapter.

## 2.2 Basic ATD Implementation

It is convenient, although not always accurate, to think of an ATD implementation as shown in Figure 2.1 [1].

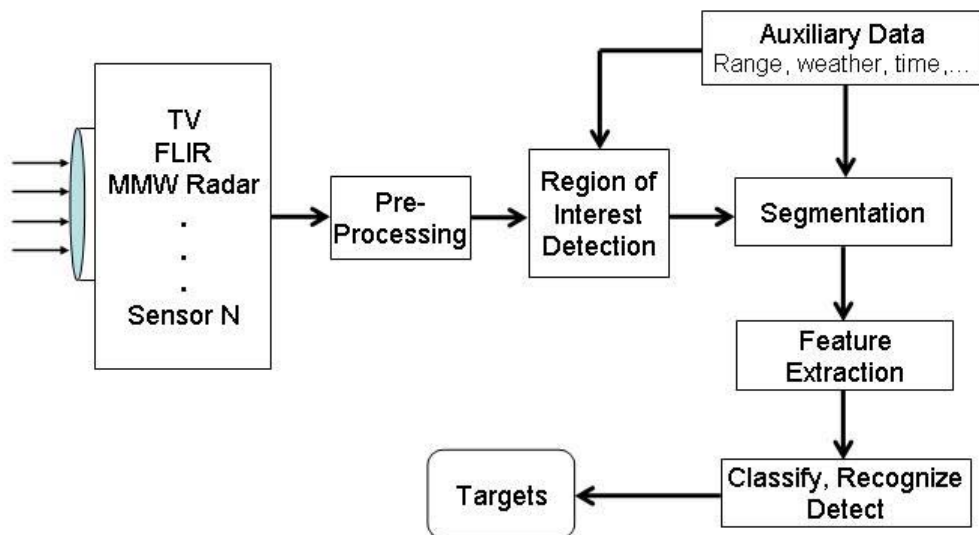


**Figure 2.1** Typical processing steps for an ATD from the sensor to target discrimination.

The scene is imaged by some sensor(s) and converted into a signal to be processed. Preprocessing step is designed to reduce clutter present in the image. Then the processor performs operations that permit detection of a region of interest and segmentation of that region. The processor may also receive information from other

sources, such as range from a laser rangefinder, position coordinates from GPS, and weather data. The other sources of data might provide contextual information that can be used to reject some possible objects of interest. Features are extracted from the segmented target to reduce the processing load for the decision-making step. Various levels of discrimination are then performed: detection, recognition, and classification. The location and description of one or more targets of interest are annotated on the final image to the operator.

### **2.3 Historical Development of ATD Systems**

Algorithms of the early 1980s were heuristic. Typically, region of interest detection was based on some sort of threshold, determined by the contrast of an object compared to the local background in an arbitrary box drawn around the object. For the segmentation, threshold techniques, boundary-based methods, region-based methods, and hybrid techniques, which combine boundary and region criteria were used [7]. Features were calculated on the segmented area to transform the problem from the image space to a feature space. The target was then represented in feature space as a vector whose components were the values of the defined quantities that have been measured on the segmented object. The selection of features was highly dependent on the sensor used for imaging [8]. The location of the vector in feature space determined the identification of that object as a target or not based upon an identification of the region of feature space as “target space” through the use of algorithm training via a set of “typical” data.

Classification was usually the highest level of discrimination and was based upon some sort of statistical classifier, e.g., Bayesian, k-nearest neighbor, nearest mean classifier. Performance of these early ATD systems was found to be marginal. Detection in low clutter did not exceed 70 percent, and recognition was little better than that obtained by random guessing. False-alarm rates in all but the most benign clutter were unacceptable [1].

The performance shortcomings of the early systems can be attributed to choice of target features. The statistical distribution of these features was measured or assumed, and thresholds were chosen for statistical classifiers. Guesses based upon intuition were made by the algorithm designer as to what features needed to be calculated that would permit separation of targets from background and each other with high probability. No understanding or analysis of the scene content or the physics behind the image formation was used or available. ATD performance degraded significantly when new targets or different environmental conditions were encountered beyond the set used to train the algorithms. These first, threshold based statistical ATD algorithms were not robust [1].

In the late 1980s and into the 1990s, a new generation of algorithms was developed that did not necessarily follow the traditional sequential processing paradigm outlined in Figure 2.1. These algorithms used knowledge-based systems or template-matching approaches. The operation of this class of algorithms can be divided into two stages: a region-of-interest (ROI) generation stage and a target identification stage. The task of the ROI stage is to locate all target-sized objects above some minimum contrast in the image. Typically, the ROIs produced by this stage are then subjected to a template matcher in which the contents of the inner window are compared to stored templates of the target set, after adjustment for pose and scale. The best match, usually in a mean-squared-error sense, is identified as the object in the ROI. Each match between an ROI and a template results in a score that can be subjected to a thresholding procedure for false-alarm reduction.

Performance of the advanced ATD systems has shown a significant increase. Detection has increased to the 80 percent level in low to medium clutter conditions. However, the false alarm rate is still high. The major improvement made in performance has been in classification and recognition.

The newest approach for increasing performance of algorithms is through the use of independent information, such as that available from multisensors, as well as integration of spatial and temporal information. The use of a model-based approach

[19] integrated with more human-like, perceptual processing neural networks is now under evaluation as a possible approach for information integration [20].

### 2.4 Proposed ATD System

In order to describe and test the methodology used in the thesis, a simple ATD system is given in this section. Details of the system are described for the blocks given in Figure 2.2 and the algorithms used in each block are chosen based on simplicity.

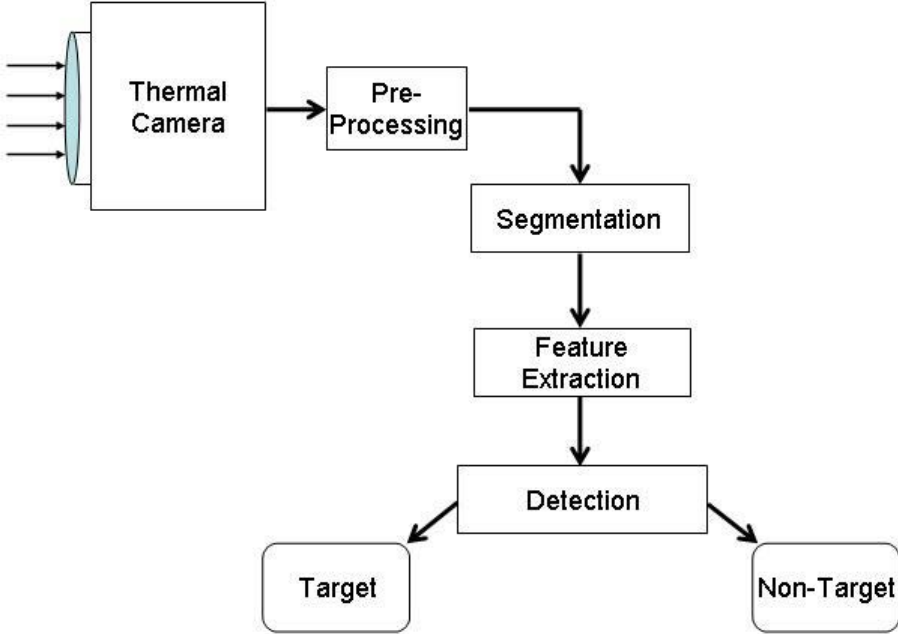


**Figure 2.2** Processing steps for proposed ATD system.

#### 2.4.1 Preprocessing

Median filter with 3x3 window size is used as prefilter because of its edge preservation property [4]. Figure 2.3 and Figure 2.4 shows an example of median filtering on a sample frame.



**Figure 2.3** Image before median filtering.



**Figure 2.4** Image after median filtering.

### **2.4.2 Segmentation**

Used algorithm for segmentation stage of the ATD system is “seeded region growing” which is based on the conventional region-growing postulate of similarity of the pixels within regions [7].

Seeded region growing (SRG) performs a segmentation of an image with respect to a number of seeds which have been grouped into  $N$  sets,  $A_1, A_2, A_3, \dots, A_N$ . It is in the choice of seeds that the decision of what is a feature of interest and what is irrelevant or noise is embedded. Given the seeds, SRG then finds a tessellation of the image with the property that each connected component of a region meets exactly one of the  $A_i$  and subject to this constraint the regions are chosen to be as homogeneous as possible. It is the application, which determines the seed sets and the homogeneity criteria. Taking into consideration that image sequences used in this work are obtained by a thermal camera, which works on “black hot” mode, (hotter objects are seen darker) one set of seed points is used. Then segmentation algorithm works as below:

- Take pixels, whose intensity value is between “upper seed threshold” -135- and “lower seed threshold” -75- as the seed set.
- Label seed points as target.
- Put seed points in a buffer.

*While the buffer is not empty:*

- Remove first point “y” from the buffer,
- Test the neighbors of the point y:

*If the neighbor satisfies intensity homogeneity criteria:*

$abs(Neighbor-y) < 15$  (“Grow Threshold”) and  $(Neighbor < 170$   
“Target Upper Bound Intensity”)

- Label the pixel as target
- Add the neighbor point to the buffer

With seeded region growing, if the regions are relatively noiseless, all that is necessary, for a good segmentation is that each seed pixel has a gray value, which is typical of its region. Upper, lower seed thresholds, target upper bound intensity and grow threshold are determined intuitively. Figure 2.5, Figure 2.6 and Figure 2.7 show the results of this segmenter on a sample frame.



**Figure 2.5** Image before segmentation.



**Figure 2.6** Seed points labeled with white color.



**Figure 2.7** Segmented image.

### 2.4.3 Feature Extraction

#### 2.4.3.1 Connected Component Labeling

Before extracting features, target pixels must be clustered into connected regions, which are the shapes in the image. Connected components labeling algorithm scans an image and groups its pixels into components based on pixel connectivity, i.e. all pixels in a connected component share similar pixel intensity values and are in some way connected with each other.

#### 2.4.3.2 Feature Selection

Size, intensity and shape-based features of segmented objects are used for classification purpose in thermal camera sequences [18]. Three image sequences are used as training database for classification. These sequences were obtained by a thermal camera and selected to cover image and target signature variability as much as possible. 25Hz sampled frames of these sequences are downsampled by 1/40 in order to reduce workload. Groundtruth to obtain feature values are drawn by hand and frames of these sequences contain at most one target.

**Table 2.1** Thermal Image Sequences

<b>Sequence Name</b>	<b>Frame Number</b>	<b>Frame Size (pixel x pixel)</b>
Thermal09	85 frames	288x360
Thermal08	31 frames	288x360
Thermal07	84 frames	288x360

### 2.4.3.2.1 Size Features

Target area, target minimum bounding rectangle (MBR) area and target perimeter are the size features that are used.

Target Area is the count of pixels belonging to target, obtained from hand drawn groundtruth image. Target area values and some statistical values about this feature for the image sequences are given in Figure 2.8 and Table 2.2.

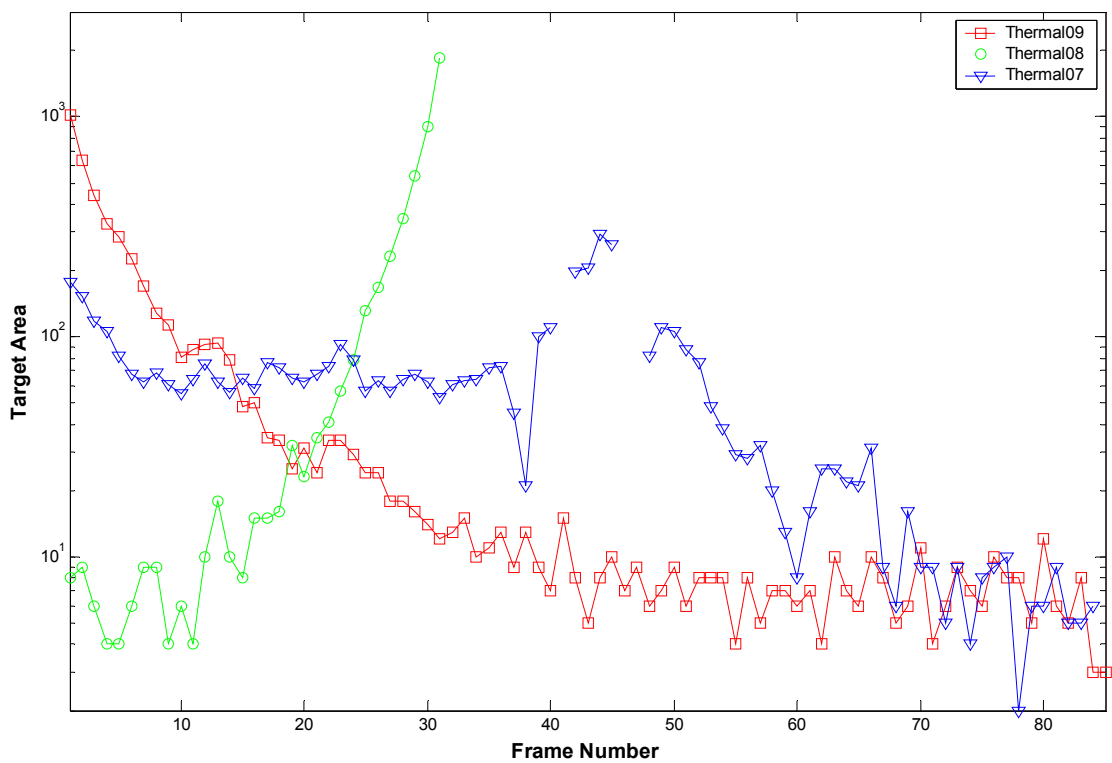
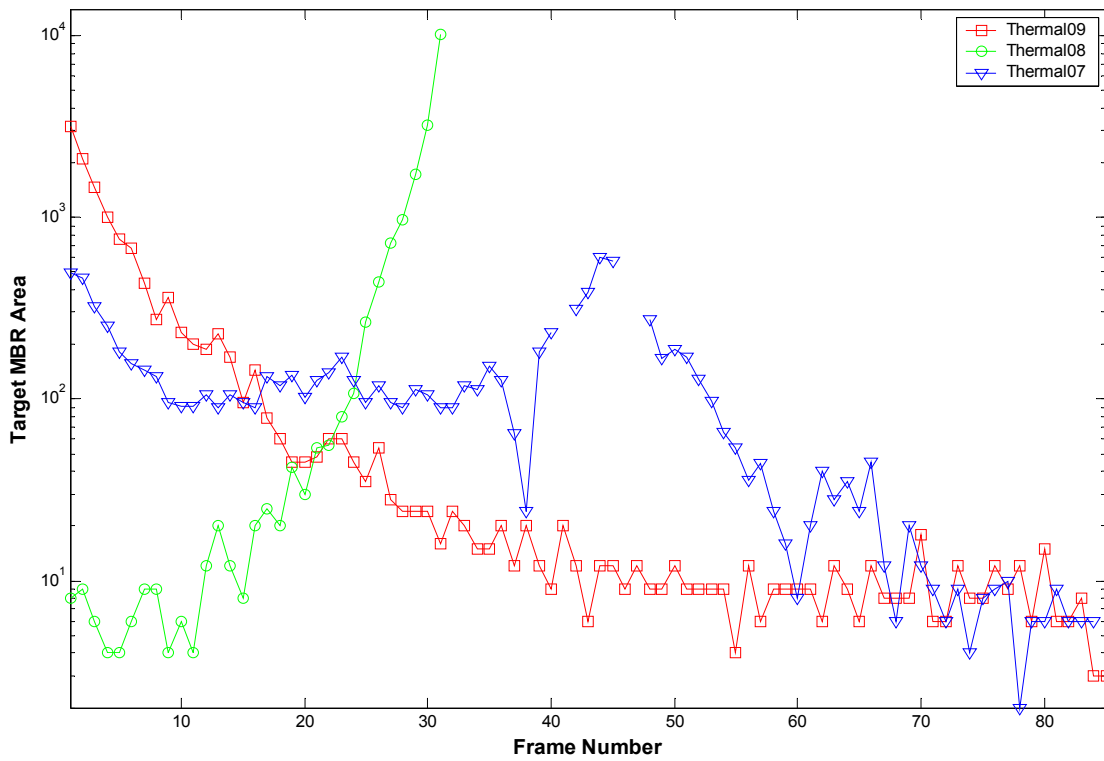


Figure 2.8 Target area values of thermal camera sequences 09-08-07.

**Table 2.2** Target Area Statistics

Sequence Name	Mean of Target Area	Std of Target Area	Minimum Target Area	Maximum Target Area
Termal07	57.8	55.6	1	291
Termal08	148.3	368.5	4	1848
Termal09	55.0	143.6	3	1019

Target MBR Area is the count of pixels belonging minimum rectangle that bounds target obtained from hand drawn groundtruth image. MBR area values and some statistical values about this feature for the image sequences are given in Figure 2.9 and Table 2.3.



**Figure 2.9** Target MBR area values of thermal camera sequences 09-08-07.

**Table 2.3** Target MBR Area Statistics

Sequence Name	Mean of MBR Area	Std of MBR Area	Minimum MBR Area	Maximum MBR Area
Termal07	110.2	125.4	1	600
Termal08	580.0	1882.9	4	10089
Termal09	149.7	445.2	3	3159

Perimeter is the count of pixels belonging boundary of the target obtained from hand drawn groundtruth image. Perimeter values and some statistical values about this feature for the image sequences are given in Figure 2.10 and Table 2.4.

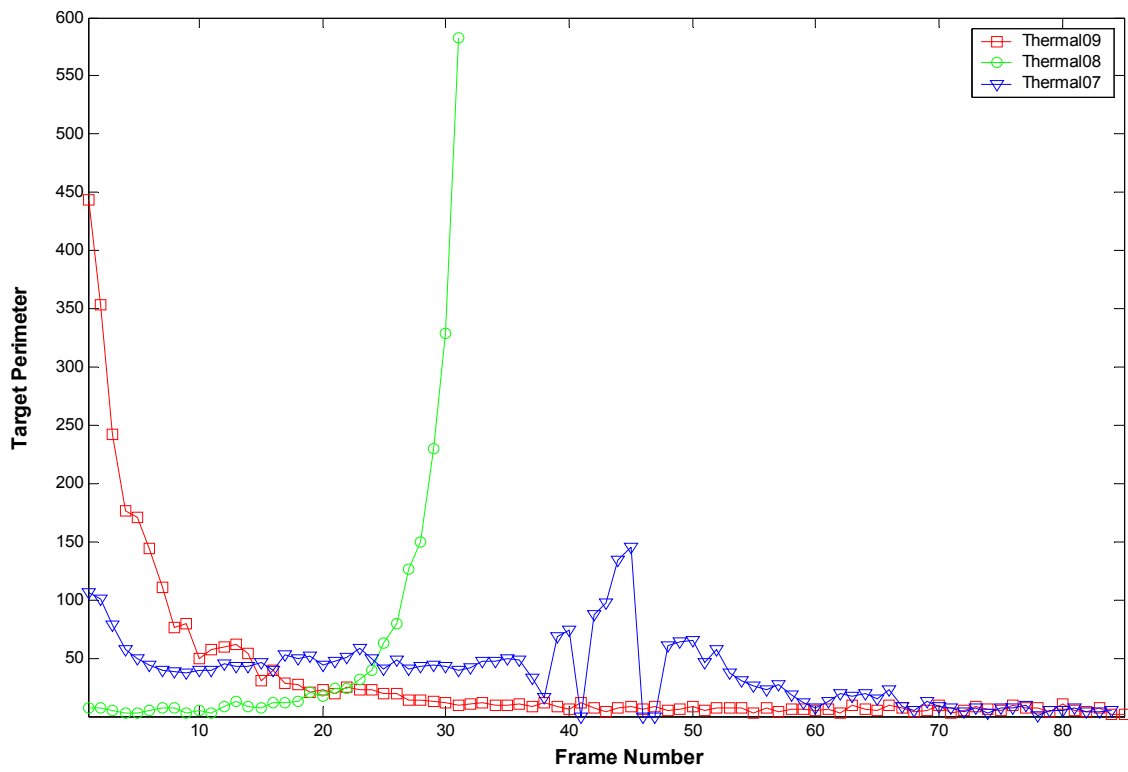


**Figure 2.10** Target perimeter values of thermal camera sequences 09-08-07.

**Table 2.4** Target Perimeter Statistics

Sequence Name	Mean of Target Perimeter	Std of Target Perimeter	Minimum Target Perimeter	Maximum Target Perimeter
Termal09	33,9	70,7	3	444
Termal08	60,4	121,6	4	583
Termal07	38,1	29,5	1	146

### 2.4.3.2.2 Shape Features

Aspect ratio and Area/MBR Area ratio are the shape features that are used. Aspect ratio is the ratio of the width of the target MBR to the height. Aspect ratio values and some statistical values about this feature for the image sequences are given in Figure 2.11 and Table 2.5.

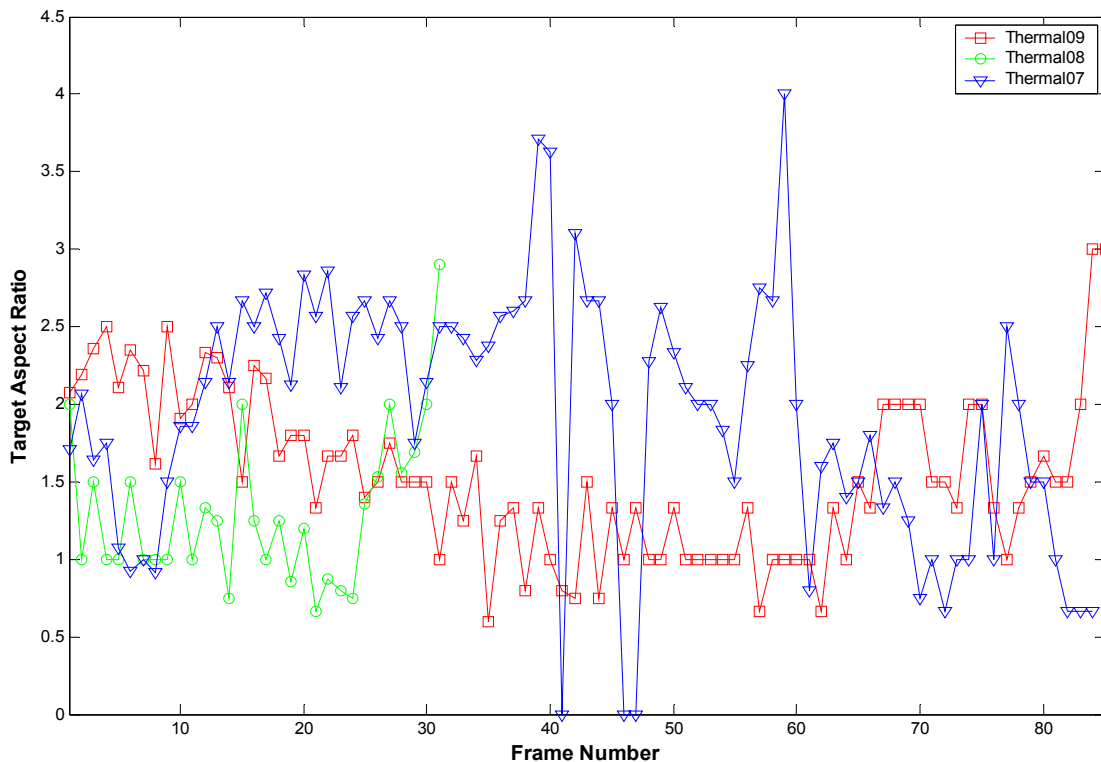


**Figure 2.11** Target aspect ratio values of thermal camera sequences 09-08-07.

**Table 2.5** Target Aspect Ratio Statistics

Sequence Name	Mean of Target Aspect Ratio	Std of Target Aspect Ratio	Minimum Target Aspect Ratio	Maximum Aspect Ratio
Termal09	1,54	0,53	0,5	3
Termal08	1,30	0,49	0,66	2,9
Termal07	1,92	0,81	0,66	4

Area/MBR Area ratio is the ratio of the target area to the target MBR area. Area/MBR Area ratio values and some statistical values about this feature for the image sequences are given in Figure 2.12 and Table 2.6.

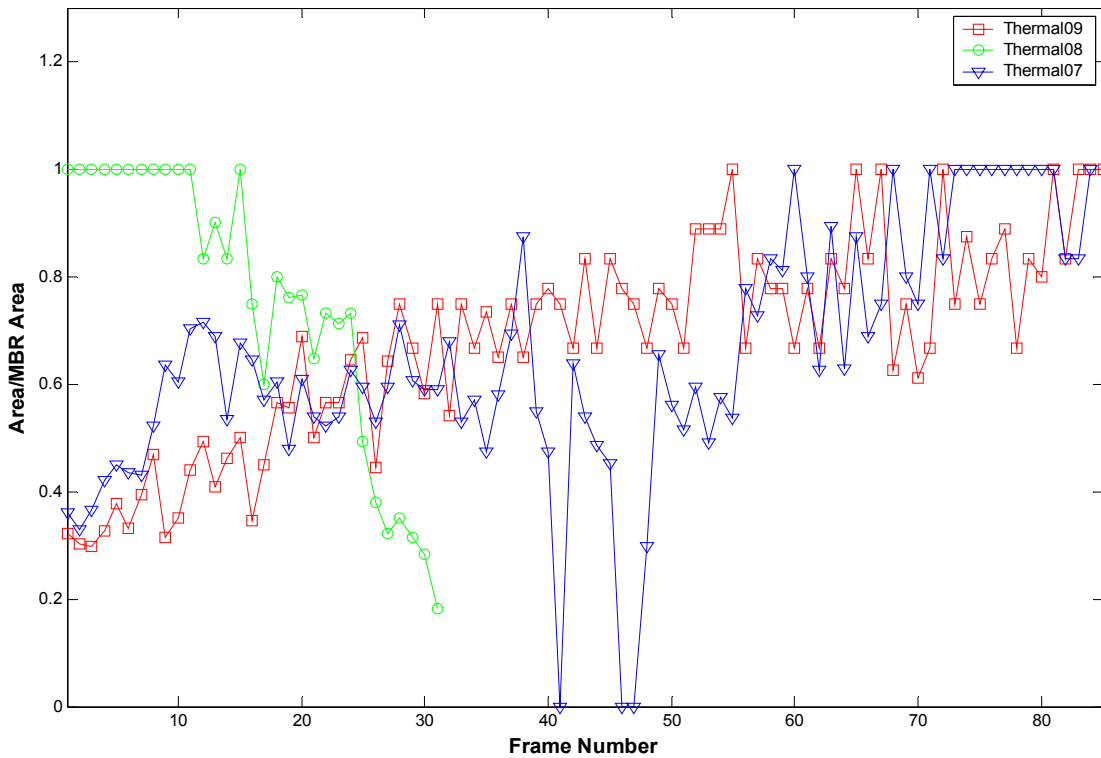


**Figure 2.12** Target Area/MBR Area ratio values of thermal camera sequences 09-08-07.

**Table 2.6** Target Area/MBR Area Ratio Statistics

Sequence Name	Mean of Target Area/MBR Area	Std of Target Area/MBR Area	Minimum Target Area/MBR Area	Maximum Target Area/MBR Area
Termal09	0,68	0,19	0,29	1
Termal08	0,75	0,26	0,18	1
Termal07	0,64	0,22	0,34	1

#### **2.4.3.2.3 Intensity Features**

Target intensity mean and target intensity standard deviation are the intensity features that are used.

Target intensity mean is the statistical mean of the target intensity. Target intensity mean values and some statistical values about this feature for the image sequences are given in Figure 2.13 and Table 2.7.

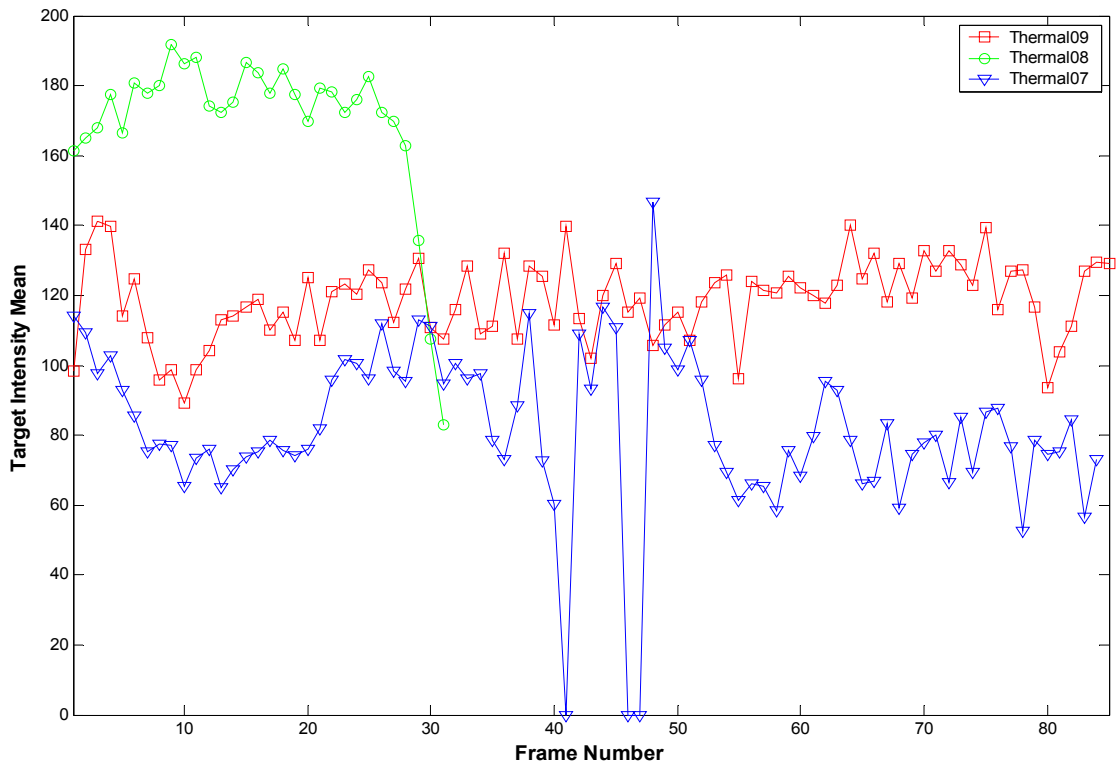


**Figure 2.13** Target intensity mean values of thermal camera sequences 09-08-07.

**Table 2.7** Target Intensity Mean Statistics

Sequence Name	Mean of Target Mean Intensity	Std of Target Mean Intensity	Minimum Target Mean Intensity	Maximum Target Mean Intensity
Termal09	118,6	11,4	89,3	141
Termal08	169,8	22,7	83	191,7
Termal07	81,7	23,3	57,6	146,5

Target intensity standard deviation (std) is the statistical standard deviation of the target intensity. Target intensity std values and some statistical values about this feature for the image sequences are given in Figure 2.14 and Table 2.8.

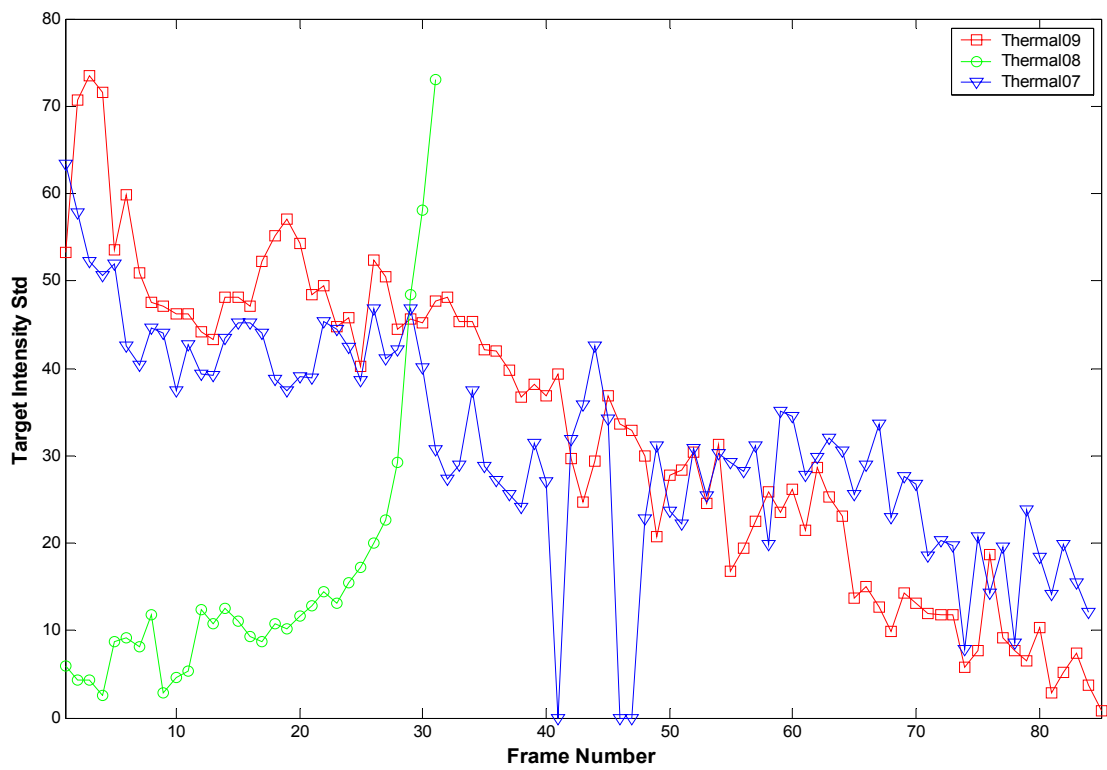


**Figure 2.14** Target intensity std values of thermal camera sequences 09-08-07.

**Table 2.8** Target Intensity Standard Deviation Statistics

Sequence Name	Mean of Target Intensity Std	Std of Target Intensity Std	Minimum Target Intensity Std	Maximum Target Intensity Std
Termal09	33,0	17,7	0,81	73,4
Termal08	15,8	16,0	2,5	73,0
Termal07	31,4	12,6	7,5	63,3

#### 2.4.4 Classification

The classification stage of the proposed system identifies the segmented objects as “target” and “non-target”. Although a number of classification methods exist [21] a simple one, nearest-mean classifier, is used for classification. Nearest mean classifier calculates the centers of in-class and out-of-class training samples and then assigns the upcoming samples to the closest center. It can model compact distributions effectively. This classifier gives distance values at its output. Seven features and mean values of these features obtained from training database are used to constitute in-class vector mean of the “target” objects (Table 2.9).

**Table 2.9** Training Database Statistics

		Mean	Std	Min	Max
<i>Size Features</i>	Area	87,0	189,2	2	1846
	MBR Area	297,9	821,2	2	1089
	Perimeter	44,2	73,9	2	583
<i>Shape Features</i>	Aspect Ratio	1,59	0,61	0,6	4
	Area/MBR Area Ratio	0,69	0,23	0,30	1
<i>Intensity Features</i>	Mean Intensity	123,3	19,1	57,6	191,7
	Std Intensity	26,7	15,4	0,81	73,4

Distance of the objects under consideration (target candidates) from training “target” mean is obtained according to the equation 2.1. Coefficients are used to give weights to the features and can be determined regarding the application. In this work they are determined with some kind of reliability criteria -inverse proportional to standard deviation values of the features obtained from training database (Table 2.10)-.

$$Distance = \left[ Coeff1 \times \frac{(TF1 - F1\_Mean)}{F1\_Mean} + \dots + CoeffN \times \frac{(TFN - FN\_Mean)}{FN\_Mean} \right] \quad (2.1)$$

where  $TFN$  is  $N$ th target feature value of candidate object and  $FN\_Mean$  is the mean value obtained with training database.

**Table 2.10** Distance Coefficients

			Std/Mean Ratio	(Std/Mean Ratio) <sup>-1</sup>	Feature Coefficient
<b>Thermal Camera Sequences</b>	<i>Size Features</i>	Area	2,17	0,46	0,0297
		MBR Area	2,75	0,36	0,0232
		Perimeter	1,67	0,60	0,0387
	<i>Shape Features</i>	Aspect Ratio	0,38	2,63	0,1698
		Area/MBR Area Ratio	0,33	3,03	0,1956
	<i>Intensity Features</i>	Mean Intensity	0,15	6,66	0,4300
		Std Intensity	0,57	1,75	0,1130

### 2.4.5 Decision

Objects under consideration (target candidates) are declared as valid targets regarding two criteria:

- Min/Max values: If *one of the* object features is out of the range of training database values (i.e higher than the Target Intensity Mean maximum value or lower than the Target Intensity Mean minimum value) the object is defined as non-target object.
- Distance Value: If the object is not defined as non-target according to the Min/Max values, its distance value (equation 2.1) is compared with a threshold (“classification threshold”). The object is declared as valid-target if its distance value is lower than threshold value. The threshold is determined regarding required probability of detection and tolerable false alarm rate.

### 2.4.6 Performance Evaluation

Three performance metrics are generally used for performance evaluation of ATD systems [18].

- Probability of Detection: If valid-target object centroid is inside the valid region of the groundtruth object it is declared as “detected target”. Valid region of groundtruth is the circle whose radius is determined by square root of the area of the groundtruth target and whose centre is determined by the groundtruth centroid. The ratio of the detected targets to total targets in the image gives us the probability of detection. In this approach there may be more than one valid-target objects inside the valid region of groundtruth. In this case valid-target with largest area is declared as detected target. Different valid area specifications can be made regarding the application but this is not in the scope of this work.

- False Alarm Rate: Number of valid-targets that are not declared as detected target is used as false alarm rate.
- Segmentation Accuracy: Ratio of the number of the common pixels between groundtruth and detected-target to the area of the groundtruth is used as segmentation accuracy performance metric.

## CHAPTER 3

### IMAGE METRICS FOR ATD SYSTEMS

#### 3.1 Introduction

Image metrics are used to characterize the image for the proposed ATD system. They are the independent variables of performance prediction models and selected specifically to the performance measure that is modeled. Many ATD metrics have been proposed in the literature. These metrics can be classified in terms of their functional dependencies (Table 3.1). ATD metrics depend on either global image statistics -those derived from the set of all pixels in the image- or regional statistics -those derived from the individual regions of a segmented image [9][10][13][14].

**Table 3.1:** Taxonomy of ATD Metrics.

	Target Independent Metrics		Target Dependent Metrics
Grey-Level	Global	Regional	Regional
Edge	Global	Regional	Regional
Size/Shape			Regional

The statistics are gathered either from the gray-level (light intensity) image directly or from an edge-map of the image. Some ATD metrics depend on a priori information about actual targets in an image to be characterized. Most of these must know the exact pixel sets containing targets. Target dependent ATD metrics are necessarily regional. Some depend on the size or shape of regions as well as gray-

level or edge information. Target independent ATD metrics may be either global or regional but depend only on gray-level or edge statistics.

In the next three sections, image metrics that will be used for building performance models are reviewed. Sections 3.2 and 3.3 concern target independent metrics and section 3.4 concerns target dependent metrics.

### 3.2 Global Image Metrics

Global image metrics are functions of all the pixels in an image. Some are dependent on all pixel values and others are dependent on edge pixels alone. Since segmentation algorithm that is used in the proposed ATD system is region based, grey-level dependent global image metrics are used heavily. Table 3.2 lists these metrics.

**Table 3.2:** Global Image Metrics.

<b>Grey-level dependent</b>	
3.2.1.1	Image gray-level standard deviation
3.2.1.2	Image gray-level entropy
3.2.1.3	Image gray-level uniformity
3.2.1.5	The spread of the main diagonal of the co-occurrence matrix
<b>Edge dependent</b>	
3.2.1.6	Information content of an image

#### 3.2.1 Gray-Level Dependent

Most of the global gray-level metrics in the literature depend on contrast and uniformity. The two simplest of these, the standard deviation of an image and the entropy of its histogram are shown in Figure 3.1 and Figure 3.2. Standard deviation (std) of the image is calculated according to Equation 3.1.

$$Std = \left[ \frac{1}{n-1} \sum_{i=1}^n (x_i - \bar{x})^2 \right]^{1/2} \quad (3.1)$$

where

$$\bar{x} = \frac{1}{n} \sum_{i=1}^n x_i \quad (3.2)$$

and  $n$  is the number of the pixels in the image and  $x_i$  is the intensity value of the individual pixel.

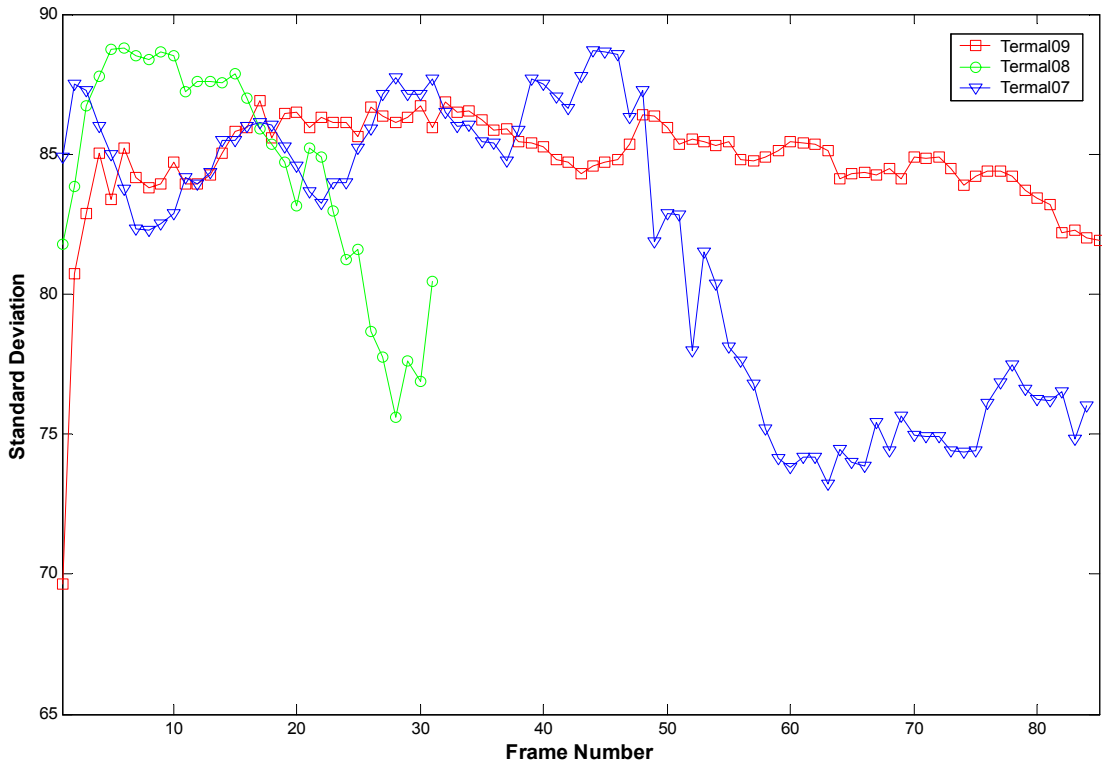


**Figure 3.1** Grey-Level standard deviation of thermal camera sequences 09-08-07.

Entropy is a measure of information content. One way to apply the concept of entropy to databases in general and histogram specifically is to consider the information being “transmitted” as the data distribution of the attribute value in question within one bucket. The more important a certain data value is, the higher will be its frequency. Assuming  $N$  is the sum of frequencies of all data values

within one bucket, the probability of a data value is  $n_i/N$  where  $n_i$  is the frequency associated with that data value. Then entropy for an image is defined as:

$$Entropy = -\sum_{i=1}^{255} \frac{n_i}{N} \log \frac{n_i}{N} \quad (3.3)$$

where  $n_i$  is the total number of pixels whose intensity value is equal to  $i$  and  $N$  is the total number of pixels in the image.

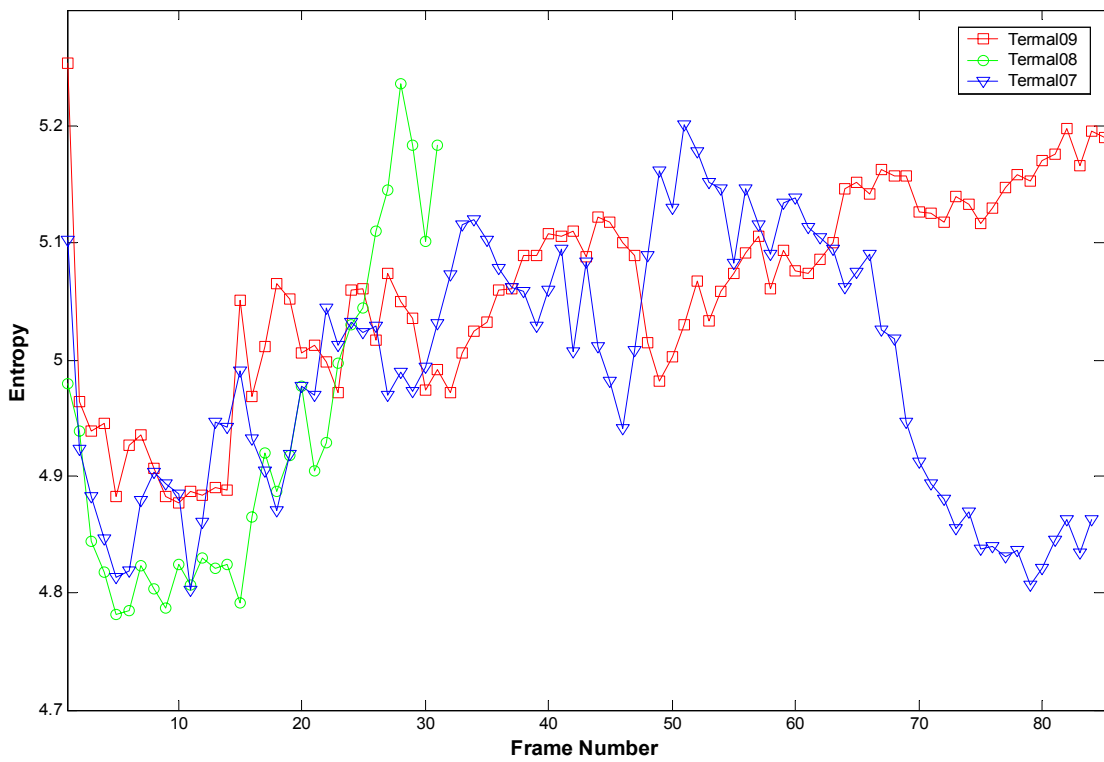


**Figure 3.2** Gray-Level entropy of thermal camera sequences 09-08-07.

Bhanu [10] defines the gray-level uniformity,  $U$ , to be a metric that is a global average of local gray-level homogeneity,

$$U = \sum_x \sum_y \left[ f(x,y) - f'(x,y) \right]^2 \quad (3.4)$$

where  $f(x, y)$  is the gray-level at pixel  $(x, y)$  and  $f'(x, y)$  is the average gray-level in a  $N \times N$  window centered at  $(x, y)$ . Figure 3.3 and 3.4 gives global uniformity values of training database for window sizes of  $3 \times 3$  and  $5 \times 5$ .

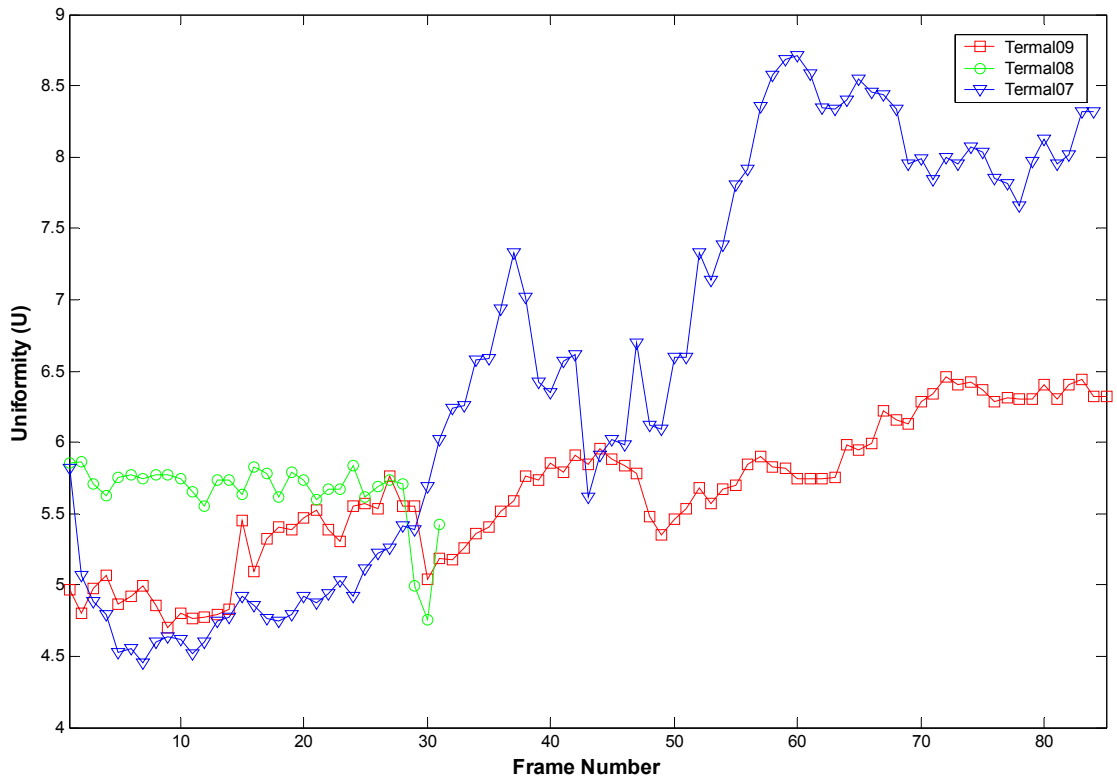


**Figure 3.3** Gray-Level uniformity (window size= $3 \times 3$ ) of thermal camera sequences 09-08-07.

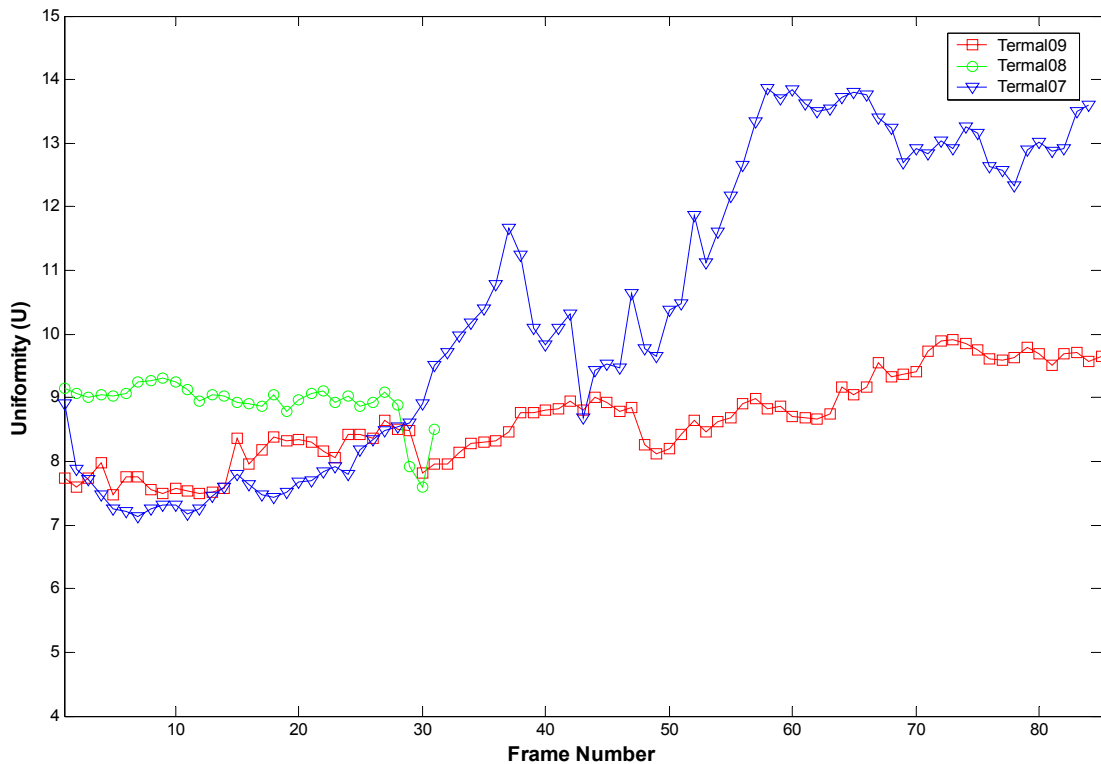


**Figure 3.4** Gray-Level uniformity (window size=5x5) of thermal camera sequences 09-08-07.

Another global gray-level metric uses the co-occurrence matrix,  $M$ .  $M$  is an  $n \times n$  matrix where  $n$  is the number of gray-levels in the image. For any pixel,  $p$ , with gray-level  $i$ , element  $m_{ij}$  of  $M$  represents the probability that one of  $p$ 's 4-neighbors has gray-level  $j$ . The main diagonal of  $M$  contains the probabilities that a pixel of gray-level  $i$  has an 8-neighbor of gray-level  $i$ . Therefore, the pixels on and near the main diagonal with some *distance* of the co-occurrence matrix contain information about the gray-level uniformity of the image (Figure 3.5 and Figure 3.6). Then occurrence matrix based global uniformity is,

$$Uniformity = \frac{\sum_{i=1}^{256} \sum_{j=1}^{256} \text{ElementsofOccurenceMatrix}\{if \_abs(i - j) < Distance\}}{\left( \sum_{i=1}^{256} \sum_{j=1}^{256} \text{ElementsofOccurenceMatrix} \right) \times 8} \quad (3.5)$$

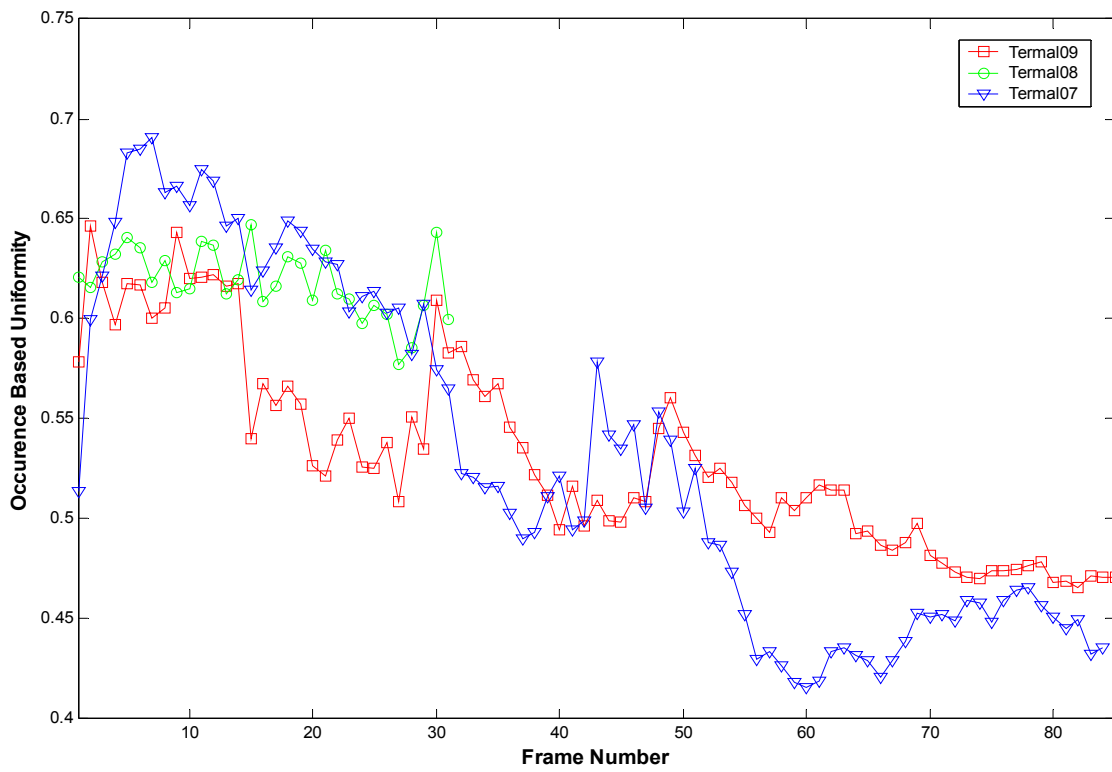


**Figure 3.5** Co-Occurrence matrix based uniformity (distance=3) of thermal camera sequences 09-08-07.

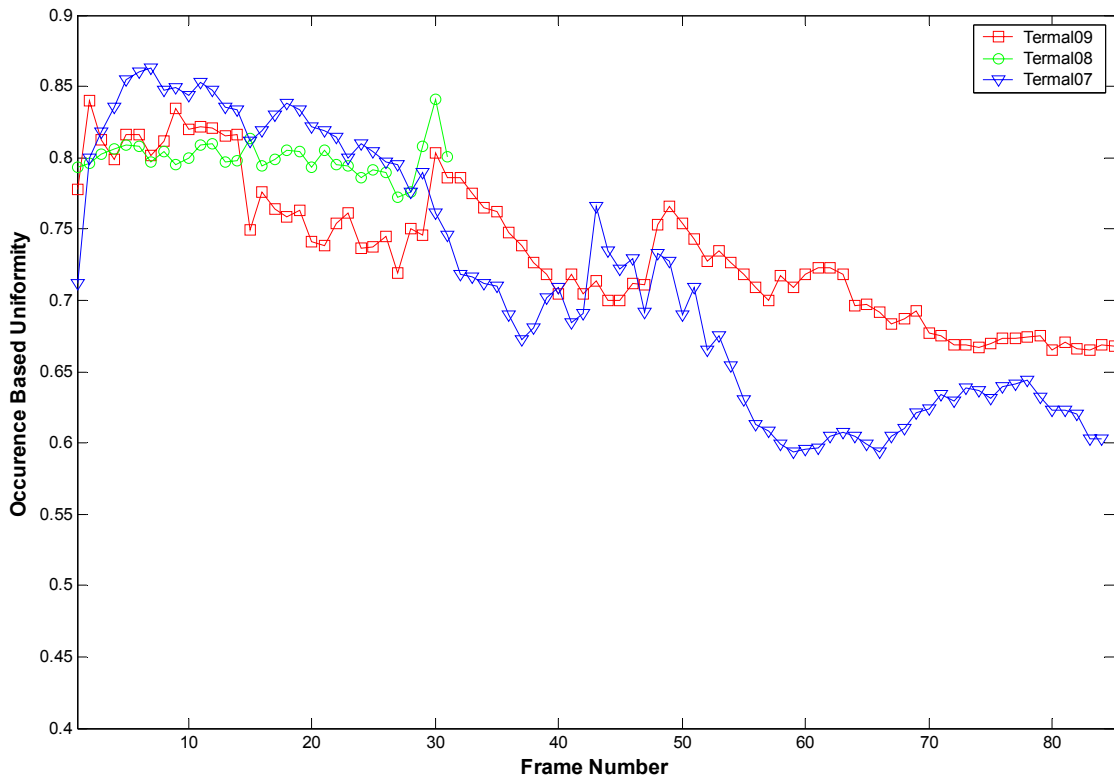


**Figure 3.6** Co-Occurrence matrix based uniformity (distance=5) of thermal camera sequences 09-08-07.

Global edge-dependent metrics measure the amount or intensity of edge activity in an image. Bhanu [10] states that since targets are usually present in the vicinity of large magnitude edge points, an image can be characterized in terms of the number of edge points whose magnitudes exceed a threshold. Given this, he claims that the number of edges exceeding a threshold per unit area in an image is a reasonable estimator of target like features. This assumes that, in general, highly textured images will present more of a challenge to an ATD than less textured images. There are finite numbers of images of a particular size that contain a given fixed number of edge points. Let  $P$  represent this number. In terms of edge pixels,

$$I = -\log_2 P \quad (3.2)$$

is the information content of the image; this is a measure of the amount of variation. Robert's edge detection operator is used for constructing edge map and edge based information content values of training database (Figure 3.7 and Figure 3.8).

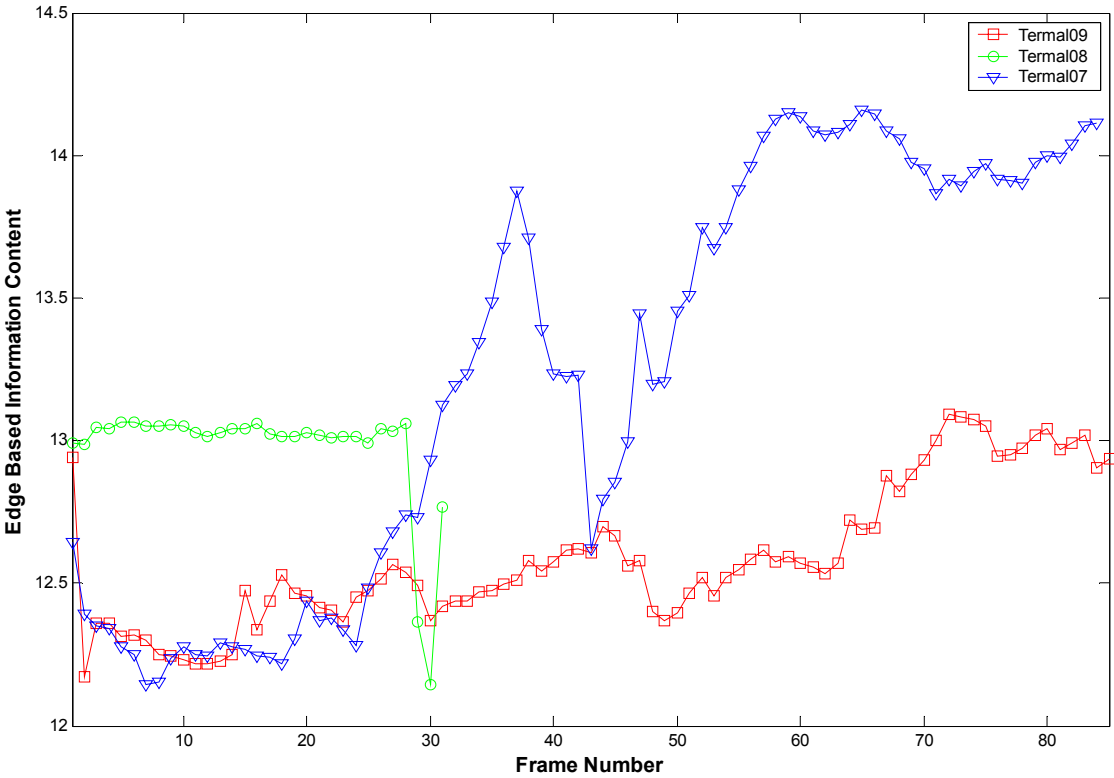


**Figure 3.7** Edge-Based information content (threshold=100) of thermal camera sequences 09-08-07.

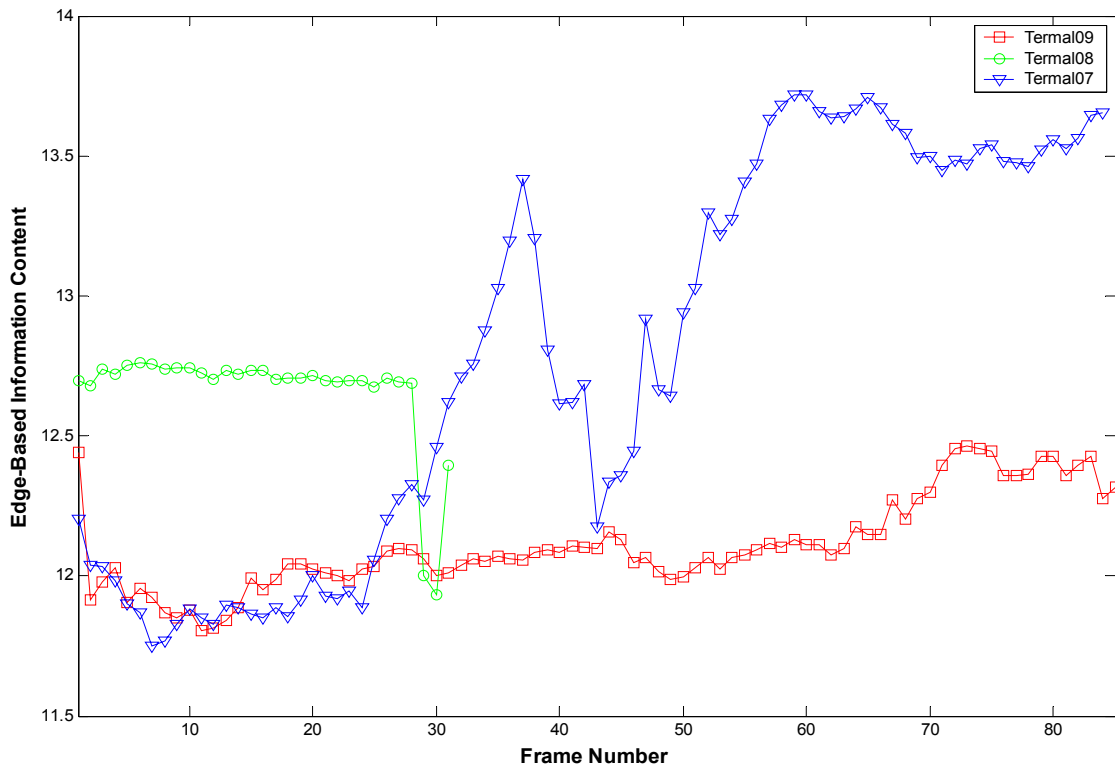


**Figure 3.8** Edge-Based information content (threshold=130) of thermal camera sequences 09-08-07.

### 3.3 Region Dependent Image Metrics

Segmentation stage of an ATD algorithm partitions the input image into regions. There have been a number of metrics devised to measure the accuracy of segmentation. Two of them are declared (Table 3.3) and values of these metrics are given for the proposed segmentation method in Figures 3.9 and Figures 3.10. Besides these metrics features defined in Section 2.4.3 can be used as region dependent metrics to give information about accuracy of segmentation to obtain targets.

**Table 3.3:** Region Dependent Image Metrics.

Grey-level dependent	
3.3.1	Regional Std
3.3.2	Local contrast

Levine and Nazif [11] have introduced a general-purpose performance measurement scheme for image segmentation algorithms. Among the gray-level characteristics the scheme measures are regional std and regional contrast.

Assume region  $R_j$  has area  $A_j$  and gray-level variance  $\sigma_j^2$  and is a subset of a larger region,  $G$ , that has area  $A_G$ . Let  $\sigma_{\max}^2$  be one half of the squared difference between the maximum and minimum gray-levels in region  $G$ . Then,

$$u_{jG} = A_j \sigma_j^2 / A_G \sigma_{\max}^2 \quad (3.3)$$

is a regional uniformity measure. It is  $R_j$ 's fraction of the maximum possible variance in  $G$  weighted by  $R_j$ 's proportion of the area of  $G$ . To use this metric it is modified as,

$$RegionalStd = \frac{A_1 \sigma_1^2 + \dots + A_j \sigma_j^2}{A_G \sigma_{\max}^2} \quad (3.4)$$

where  $A_j$  is the  $j$ th object region (only valid objects are taken into consideration) on segmented image and  $A_G$  is the area of total image.

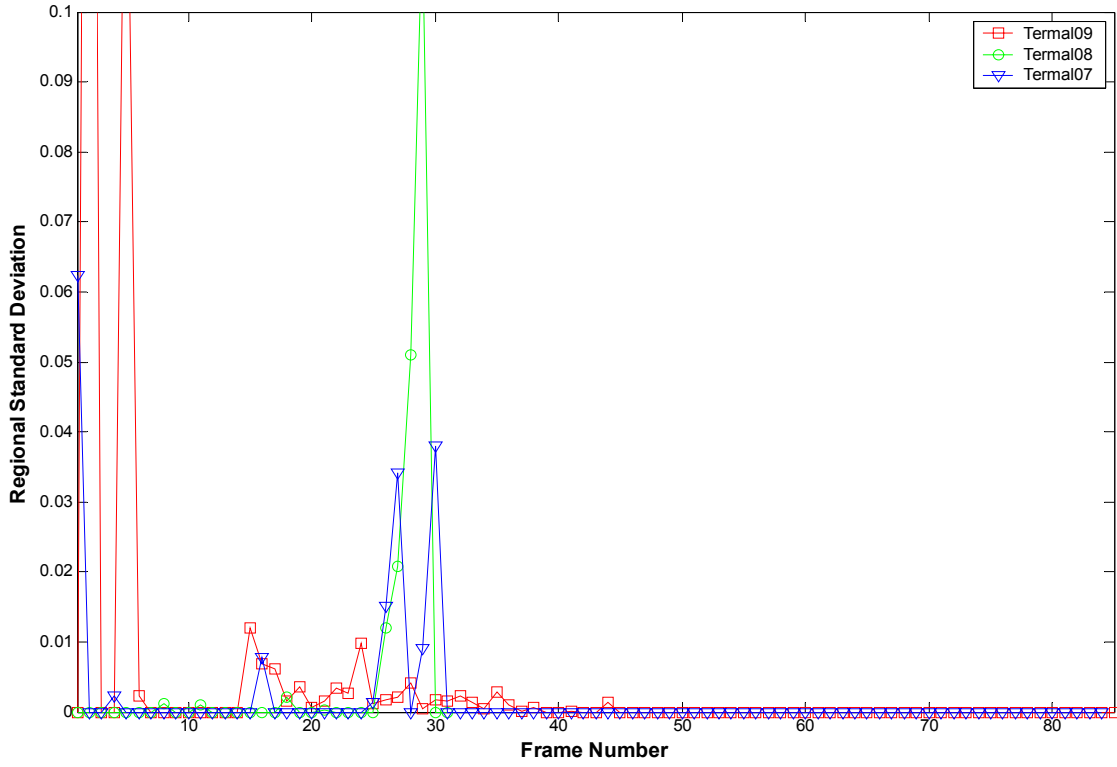


**Figure 3.9** Regional standard deviation of thermal camera sequences 09-08-07.

Levine and Nazif use the relation (3.5) to measure the local contrast between adjacent regions  $R_j$  and  $R_i$ .

$$C_{ij} = \frac{|\mu_i - \mu_j|}{|\mu_i + \mu_j|} \quad (3.5)$$

where  $\mu_i$  and  $\mu_j$  are the mean gray-levels in regions  $i$  and  $j$ . To use this metric it is modified as,

$$LocalContrast = \sum_{i=1}^n \frac{|\mu_i - \mu_G|}{|\mu_i + \mu_G|} \quad (3.6)$$

where  $\mu_i$  is the  $i$ th valid object and  $\mu_G$  is the intensity mean of the background of the image.

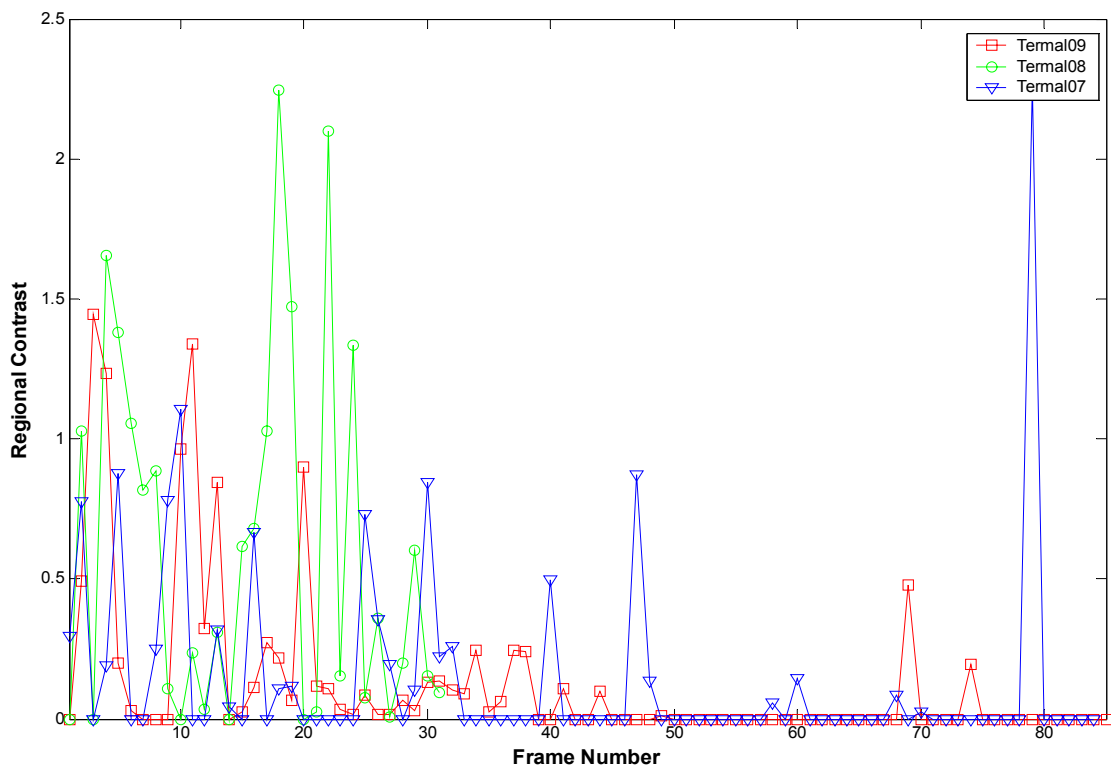


**Figure 3.10** Regional contrast of thermal camera sequence 09-08-07.

### 3.4 Target Dependent Image Metrics

The majority of ATD image metrics are target dependent. That is, they require explicit information about the location of the true targets in the image. Like the global metrics and region dependent metrics, most target dependent metrics use either gray-level or edge information. In addition to these, however, there are metrics based on target size and shape. Table 3.4 is a list of target dependent metrics that are used. Since proposed segmentation algorithm is region based, grey-level dependent metrics are preferred.

**Table 3.4:** Target Dependent Image Metrics.

Grey-level dependent	
3.4.1.1	Target Intensity Mean
3.4.1.2	Target Intensity Standard Deviation
3.4.1.3	Target to Background Contrast
3.4.1.4	Target Interference Ratio

Target intensity mean is the statistical mean of the intensity of the pixels belonging target. Target intensity standard deviation is the statistical standard deviation of the target intensity value. These target dependent metrics are also used as target features and values of them are given in Figure 2.13 and Figure 2.14.

A very simple target dependent metric is the contrast between a target and its immediate background.

$$contrast = |\mu_T - \mu_B| \quad (3.9)$$

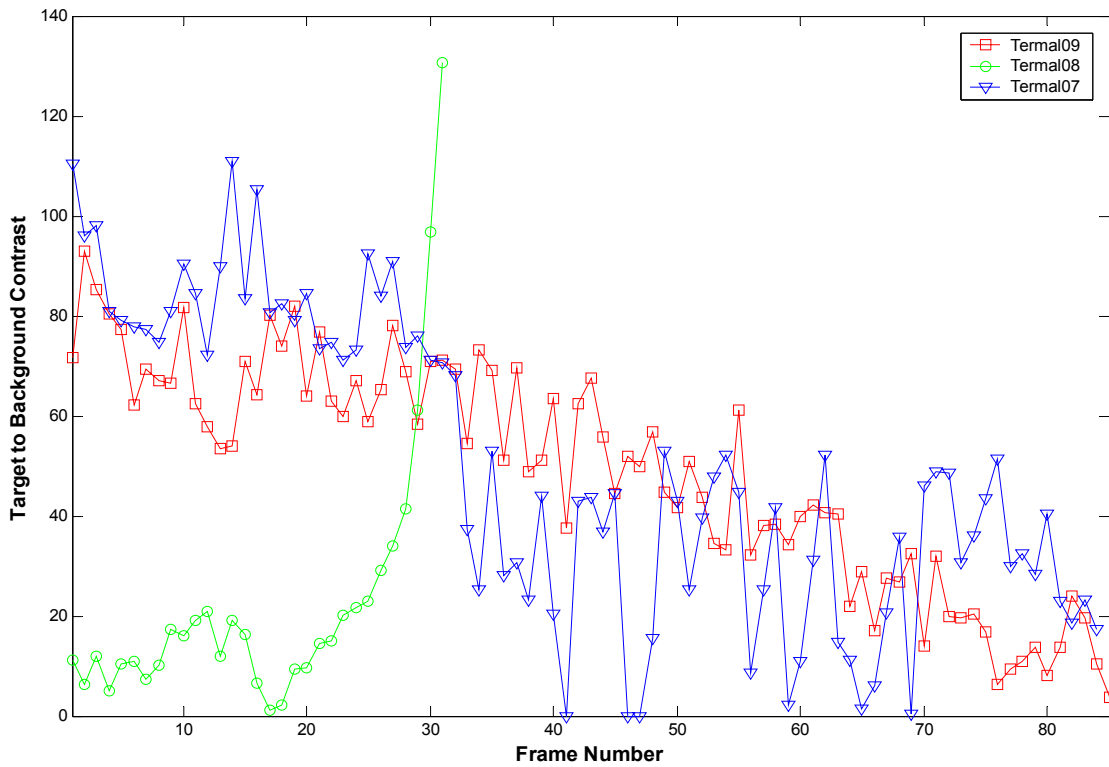


**Figure 3.11** Target to background contrast of thermal camera sequence 09-08-07.

where  $\mu_T$  is the average gray-level of the pixels in the target and  $\mu_B$  is the average gray-level of the pixels adjacent the target.

Another target dependent metric is target interference ratio. Let  $\mu_T$  and  $\sigma_T$  be the mean and standard deviation of the gray-levels inside the minimum-covering rectangle of the target. Let  $\mu_B$  and  $\sigma_B$  be the mean and standard deviation of the gray-levels inside a rectangular annulus whose inner border coincides with the target rectangle and whose outside dimensions are twice those of the target rectangle. Then the target interference ratio,

$$TIR = |(\mu_T - \mu_B)| / \sigma_B \quad (3.10)$$

indicates the separability of a target from its background. Since the metric varies inversely with the background standard deviation, it has smaller values for textured backgrounds.

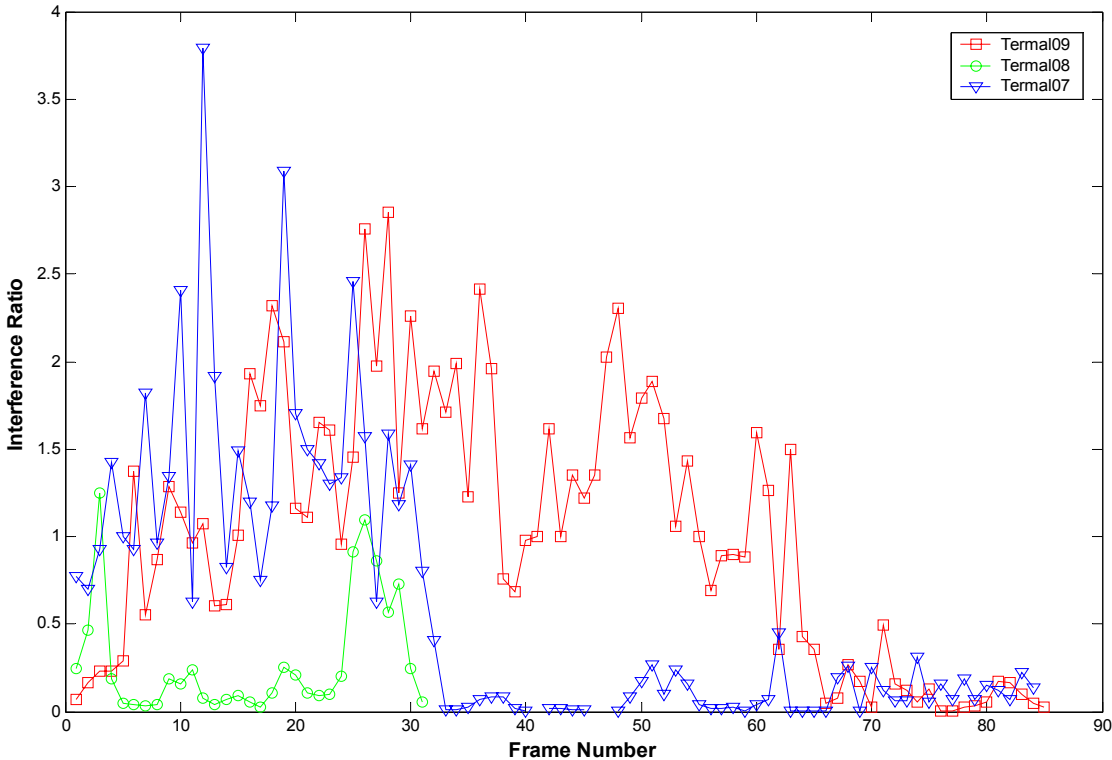


Figure 3.12 Target interference ratio of thermal camera sequence 09-08-07.

## CHAPTER 4

### EXPERIMENTAL DESIGN and PERFORMANCE MODELING

#### 4.1 Introduction

Experimental design is a very critical task in building performance prediction models. If carefully done, it can result in good and reliable models, which can ultimately result in good adaptation [3].

Performance models are formed for each performance measure (Probability of Detection - $P_D$ -, False Alarm Rate -FAR- and Segmentation Accuracy -SA-) defined in section 2.4.6. These are functions of image metrics (such as Global Uniformity) and ATD system parameters (such as Seed Grow Threshold). Given the ATD performance metric (PM), a typical model is,

$$PM = F (M_1, M_2, \dots M_N; P_1, P_2, \dots P_K) \quad (4.1)$$

where  $M_i$  ( $i=1 \dots N$ ) are image metrics and  $P_j$  ( $1 \dots K$ ) are ATD system parameters.

Performance models are generated as a result of a number of experiments. In one experiment, a set of images is selected from training sequences that corresponds to the designed experiment's image metric values. Image metrics are chosen in order to reflect those qualities that affect the ATD performance measures.

Selected images are processed by the ATD system with changing parameters, again according to the designed experiment's ATD parameter values. Used ATD system parameters are also chosen mainly due to their effects on performance measures.

Once all the images are processed through the ATD system, the parameters have been varied, and performance measure values have been collected, performance models are generated using multivariate linear regression models and the method of least squares. In other words, the performance measures, the metrics and the parameters are grouped, and a curve fit is attempted.

Second section of this chapter explains design of experiments and third section describes the process of curve fitting with these experimental designs to obtain performance models for each performance metric defined. Also obtained models are discussed in this section.

## 4.2 Design of Experiments

The problem of experimental design or design of experiments (DOE) is encountered in many fields, where, in general, the response variables of interest –PMs in this work- are  $y_1, y_2, y_m$  ( $m$  is the total number of response variables) and there is a set of predictor variables – $M_i$  and  $P_i$  in this work-  $x_1, x_2, x_n$  ( $n$  –is the total number of predictor variables). Response variables of interest are referred as responses and predictor variables as design variables or factors. A common situation for using DOE is when the designer does not know the *exact* underlying relationship between responses and design variables but wants to know how the responses are influenced by the design variables. In this case it is often helpful to approximate the underlying relationship with an empirical model:

$$y = f(x_1, x_2, \dots x_n) \quad (4.2)$$

Usually, the function  $f$  is a first- or second-order polynomial. This empirical model is called a “response surface model” (RS Model) or curve fit. To create the RS

model we need to know the value of the responses for some combinations of design variables. Each combination of design variables could be viewed as a point in the  $n$ -dimensional design space, where  $n$  is the total number of design variables. The particular arrangement of points in the design space is known as an *experimental design* or *design of experiments* [17]. The proper selection of points could drastically improve the quality of a RS model. Experimental design is dependent on the RS model and in this work “quadratic” models (equation 4.3) are preliminary proposed for performance models for design of experiments [3]. The selection of quadratic linear regression models is necessary to simplify the processes of designing experiments, curve fitting and optimization for performance measures. MATLAB software provides powerful tools for these problems.

$$y = \beta_0 + \sum_{i=1}^k \beta_i x_i + \sum_{i=1}^k \beta_{ii} x_i^2 + \sum_{i < j} \beta_{ij} x_i x_j + \varepsilon \quad (4.3)$$

One experimental design method for fitting quadratic types of models is the full factorial design having *three* values for each input. Although the Statistics Toolbox of MATLAB is capable of generating this design, it is not really a satisfactory design in most cases because it has many more runs than are necessary to fit the model after the experiments are conducted when factors of the design are relatively high (i.e. for 10 factors:  $3^{10}=59049$  experiment points).

The two most common designs generally used in response surface modeling are central composite designs and Box-Behnken designs [16]. In these designs the inputs take on three or five distinct values (levels), but not all combinations of these values appear in the design. But these designs pre-date the computer age, and some were in use by early in the 20th century. In the 1970s statisticians started to use the computer in experimental design by recasting the design of experiments (DOE) in terms of optimization. A D-optimal design is one that maximizes the determinant of Fisher’s information matrix,  $X^T X$ . This matrix is proportional to the inverse of the covariance matrix of the estimated parameters  $(\hat{\beta})$  with method of least squares according to the quadratic model defined in equation 4.3 [17].

$$\hat{\beta} = (X^T X)^{-1} X^T y \quad (4.4)$$

In this equation  $y$  is the  $n$ -by- $1$  vector of observations (from  $n$  experiments) and  $X$  is the  $n$ -by- $p$  matrix whose columns are formed by  $p$  model terms for  $n$  experiments. (See Section 4.3)

So maximizing  $\det(X^T X)$  is equivalent to minimizing the determinant of the covariance of the parameters. A D-optimal design minimizes the volume of the confidence ellipsoid of the regression estimates of the linear model parameters.

Regarding the experimental design alternatives D-optimal design method is selected for designing experiments, initially. Function of MATLAB software “cordexch” supplies D-Optimal designs with the number of design factors, maximum number of experiment points and the model that is the experiment is being done for (i.e. Quadratic). The “cordexch” function searches for a D-optimal design using a coordinate exchange algorithm. It creates a starting design, and then iterates by changing each coordinate of each design point in an attempt to reduce the variance of the coefficients that would be estimated using this design [16]. Maximum number of experiment points is selected by comparing the same design with Central Composite Design alternative (i.e. maximum than this value). One deviation from D-Optimal design is because of unobtainable experiment points (unobtainable image metric combinations) in training database. In these cases nearest points are selected instead.

Fitted models with D-Optimal designs showed that the specific characteristics of the proposed ATD algorithm make it not appropriate for D-Optimal experiment designs. Even full factorial designs with three factor levels may not be adequate because the response of ATD system (i.e. Probability of Detection) is varying between discrete values of one and zero in de facto training database (frames with one target). Unconsidered characteristics of the image (limited number of image metrics is used), errors in obtaining image metrics and experimental errors (i.e extracting groundtruth image) may easily change the performance value and it

seriously affects the experiment results when low number of experiment points is used.

Regarding these problems experimental design method is changed to increase experiment points. Range of factors (image metrics and parameters) is quantized and for these quantized values (factor levels) full factorial experimental design is conducted. This produced a large number of experiment points but also reduce all noise and unconsidered factor effects on obtained response surfaces.

Either D-Optimal experimental design points or full factorial design points are used based on the selected frames from training database that corresponds to the experimental points. Together with necessary parameters, ATD algorithm is run on selected frames and performance measures for each experimental point is obtained.

### 4.3 Performance Model Fitting

Multivariate quadratic linear regression models (equation 4.3) are used with method of least squares to estimate the regression coefficients of the models. The model given in equation 4.3 takes the common matrix form when results of the experiments ( $n$  points) are taken into consideration

$$y = X\beta + \varepsilon \quad (4.5)$$

where,

- $y$  is an  $n$ -by-1 vector of observations of response.
- $X$  is an  $n$ -by- $p$  matrix of factors (model terms).
- $\beta$  is a  $p$ -by-1 vector of model parameters.
- $\varepsilon$  is an  $n$ -by-1 vector of errors.

The solution to the problem is a vector,  $b$ , which estimates the unknown vector of parameters,  $\beta$ .

The least squares solution is:

$$b = \hat{\beta} = (X^T X)^{-1} X^T y \quad (4.6)$$

Predicted response values by the model at the experiment points are,

$$\hat{y} = Xb = Hy = X(X^T X)^{-1} X^T y \quad (4.7)$$

The residuals are the difference between the observed and predicted y values.

$$r = y - \hat{y} \quad (4.8)$$

The residuals are useful for detecting failures in the model assumptions, since they correspond to the errors,  $\varepsilon$ , in the model equation. By assumption, these errors each have independent normal distributions with mean zero and a constant variance. The residuals, however, are correlated and have variances that depend on the locations of the data points. It is a common practice to scale ("Studentize") the residuals so they all have the same variance. In the equation below, the scaled residual,  $t_i$ , has a Student's t distribution with  $(n-p-1)$  degrees of freedom

$$t_i = \frac{r_i}{\hat{\sigma}_i \sqrt{1-h_i}} \quad (4.9)$$

where

$$\hat{\sigma}_i^2 = \frac{\|r\|^2}{n-p-1} - \frac{r_i^2}{(n-p-1)(1-h_i)} \quad (4.10)$$

and

- $t_i$  is the scaled residual for the  $i$ th data point.
- $r_i$  is the raw residual for the  $i$ th data point.
- $n$  is the sample size.

- $p$  is the number of parameters in the model.
- $h_i$  is the  $i$ th diagonal element of  $H$ .

A hypothesis test for outliers involves comparing  $t_i$  with the critical values of the  $t$  distribution. If  $t_i$  is large, this casts doubt on the assumption that this residual has the same variance as the others. A confidence interval for the mean of each error is

$$c_i = r_i \pm t_{\left(1-\frac{\alpha}{2}, \nu\right)} \hat{\sigma}_i \sqrt{1-h_i} \quad (4.11)$$

Confidence intervals that do not include zero are equivalent to rejecting the hypothesis (at a significance probability of  $\alpha$ ) that the residual mean is zero. Such confidence intervals are good evidence that the observation is an outlier for the given model [17].

The coefficient of multiple determination  $R^2$  is a measure of the variability of  $y$  obtained by using the regressor variables in the model and is used throughout this work.

$$R^2 = \frac{SS_R}{SS_T} = 1 - \frac{SS_E}{SS_T} \quad (4.12)$$

where

$$SS_R = \hat{\beta}'X'y - \frac{\left(\sum_{i=1}^n y_i\right)^2}{n} \quad (4.13)$$

$$SS_E = y'y - \hat{\beta}'X'y \quad (4.14)$$

$$SS_T = y'y - \frac{\left(\sum_{i=1}^n y_i\right)^2}{n} \quad (4.15)$$

To fit the model with experiment results and get the discussed information above about the fitted model “rstoool” and “regress” functions of MATLAB software are used. These functions use Q-R decomposition to construct model information.

In following sub-sections performance models for three *performance measures* of ATD systems are fitted and examined individually.

#### 4.3.1 Probability of Detection

Evaluation of  $P_D$  for the proposed ATD algorithm is explained in Section 2.4.6. Regarding the algorithm, three target dependent image metrics and three ATD system parameters are selected as factors of the  $P_D$  response surface. (Table 4.1)

**Table 4.1** Factors for RS of Probability of Detection (D-Optimal Design)

Target Dependent Image Metrics	Target Intensity Mean	See Section 3.4
	Target Intensity Standard Deviation	See Section 3.4
	Target to background contrast	See Section 3.4
ATD Parameters	Seed Center	$= \frac{UpperSeedThreshold + LowerSeedThreshold}{2}$
	Seed Range	$= \frac{UpperSeedThreshold - LowerSeedThreshold}{2}$
	Grow Threshold	See Section 2.4.2

Parameters are selected from segmentation phase of the algorithm because of their expected effect on probability of detection. Target dependent metrics are selected although they require groundtruth knowledge because their quantities give the most important knowledge to segmentation phase of the proposed algorithm. Maximum

and minimum values for the factors are selected with regarding training database values.

Then for  $P_D$ , obtained D-Optimal experiment points and responses (Appendix A) are fitted on the model with “rstool” function of MATLAB software (Figure 4.1). “Rstool” provides interactive fit and plot of a multidimensional response surface. Graph for *each* of the factor shows the change of response variable ( $P_D$ ) when remaining factors are held constant. Constant values are shown in the boxes named with the factor name. Detection probability value on the left-hand side gives the response variable ( $P_D$ ) value for the factor values inside the boxes.

Dotted lines around the solid line of each graph show the global confidence interval for predictions. Also confidence interval for the constant values of factors (inside the boxes) is given on the left-hand side below detection probability value.

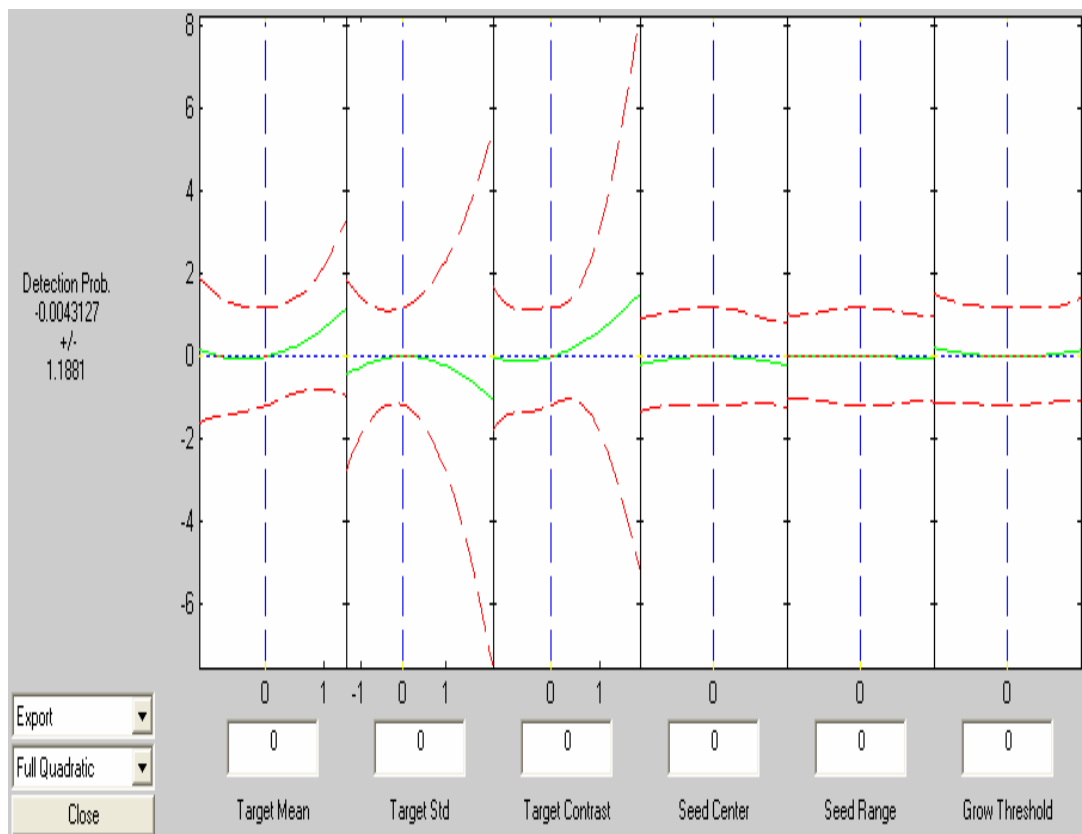


**Figure 4.1** Response surface for  $P_D$  with D-optimal experiments.

RMSE and  $R^2$  values for this model are given below:

RMSE (Root Mean Square Error) = 0.2529 (Model Dependent Standard Deviation or standard error of the regression model)

Coefficient of multiple determination ( $R^2$ ) = 0.7990.

Each residual together with its confidence interval for the mean are plotted on Figure 4.2. Residuals that do not include zero (outliers) in their confidence interval are shown in this figure.

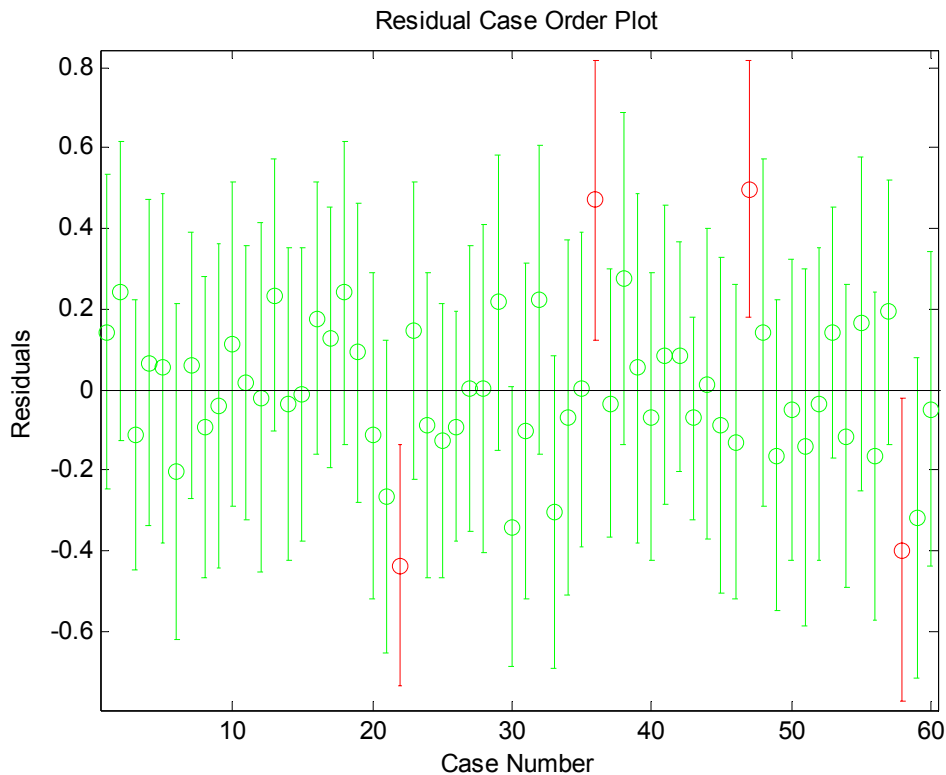


**Figure 4.2** Residual values for RS of  $P_D$  with D-optimal experiments.

Regarding information above, this model can be considered as a “good” model. But expected effects of some factors (from knowledge of the system) are not observed on this model. For this model probability of detection has negligible dependency on

ATD parameters. This is mainly because of unconsidered characteristics of the image (three target dependent metrics are used only), errors in obtaining image characteristics and experimental errors (i.e extracting groundtruth image) that effect low number of experimental results. Then experimental design is changed as explained in Section 4.2. Factors for the new RS of P<sub>D</sub> are given in Table 4.2. Factor ranges are quantized as given in Table 4.3.

**Table 4.2** Factors for RS of Probability of Detection (Full Factorial Design)

Target Dependent Image Metrics	Target Intensity Mean	See Section 3.4
	Target Intensity Standard Deviation	See Section 3.4
	Target to background contrast	See Section 3.4
ATD Parameters	Seed Center	$= \frac{UpperSeedThreshold + LowerSeedThreshold}{2}$
	Target Upper Bound Intensity	See Section 2.4.2
	Grow Threshold	See Section 2.4.2

**Table 4.3** Factor Levels for Full Factorial Design

		Target Mean	Target Std	Target Contrast	Seed Center	Target Upper Bound	Grow Contrast
Range	Min	40	0	0	25	Seed Center + 15	5
	Max	200	80	140	165	Seed Center + 45	17
Step Size		20	20	20	10	10	4

Considering these levels for full factorial design; Number of Experimental Points is equal to 76800 (=8x5x8x15x4x4) but since not the entire image metric combinations can be obtained from training database 14400 (=60x15x4x4) are used for experiments.

Then for  $P_D$ , obtained experiment points and responses are fitted on the model with “rstool” function of MATLAB software. (Figure 4.3)

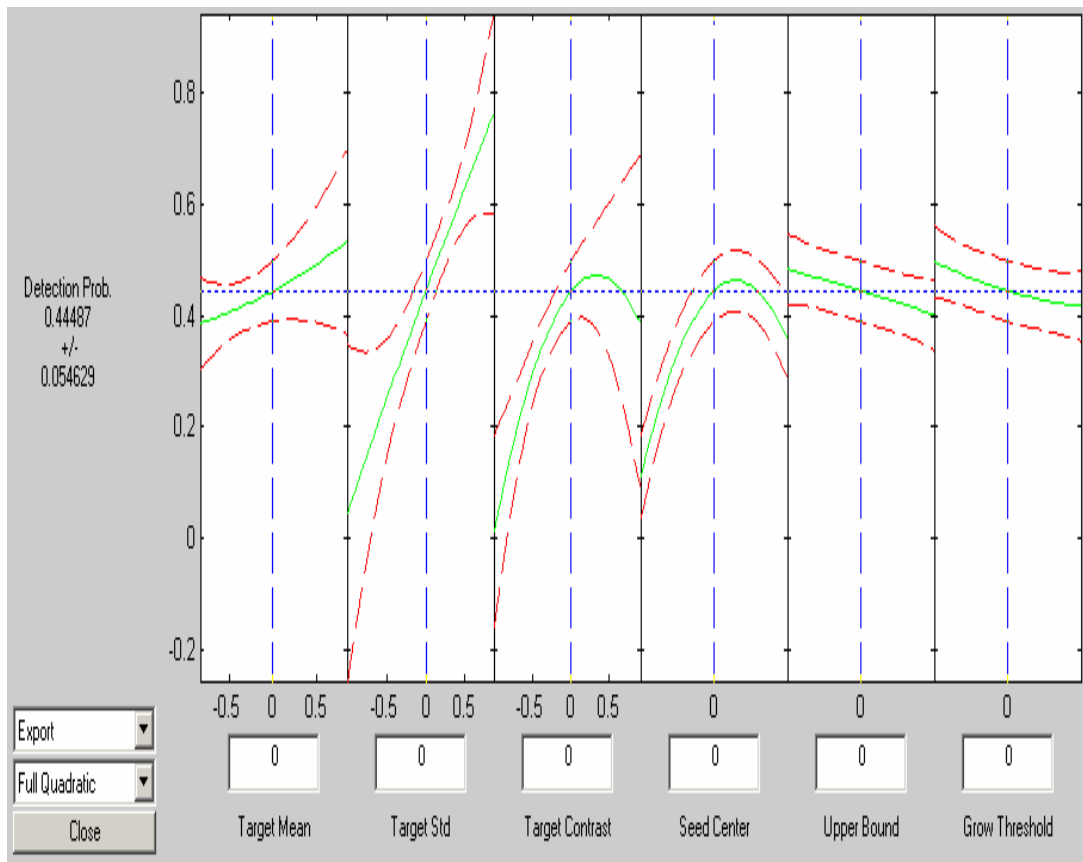


**Figure 4.3** Response surface for  $P_D$  with full factorial experiments.

RMSE and  $R^2$  values for this model are given below:

RMSE of this model is: 0.3113

Coefficient of multiple determination ( $R^2$ ) = 0.3563

Residual values from (1 to 200) and (2001 to 2201) together with their confidence intervals for the mean are plotted on Figure 4.4 and Figure 4.5. Residuals that do not include zero (outliers) in their confidence interval are show in these figures.

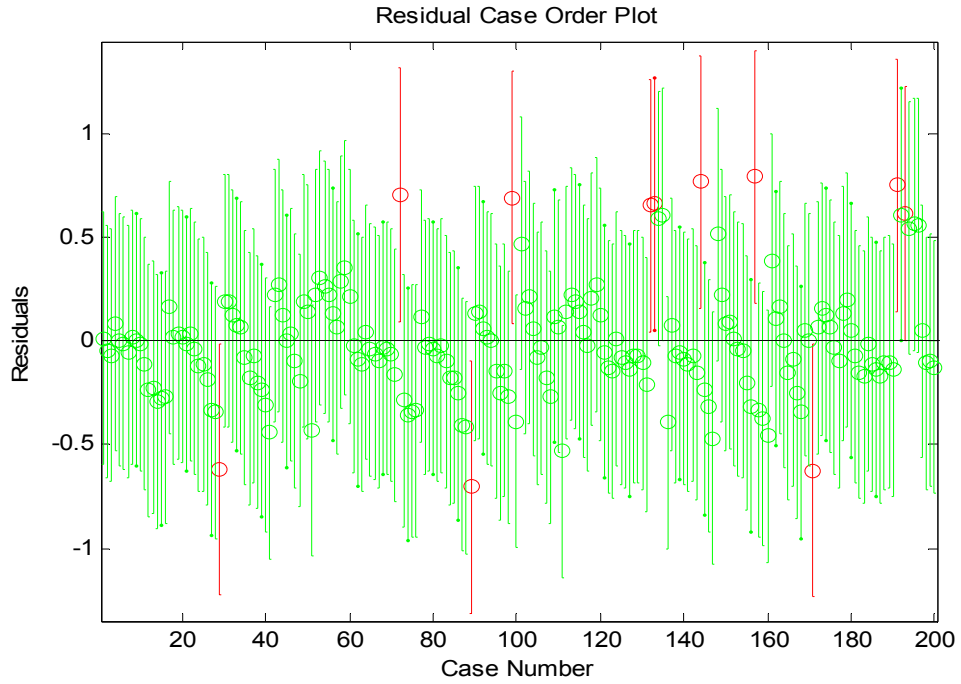


**Figure 4.4** Residual values (1 to 200) for RS of  $P_D$  with full factorial experiments.

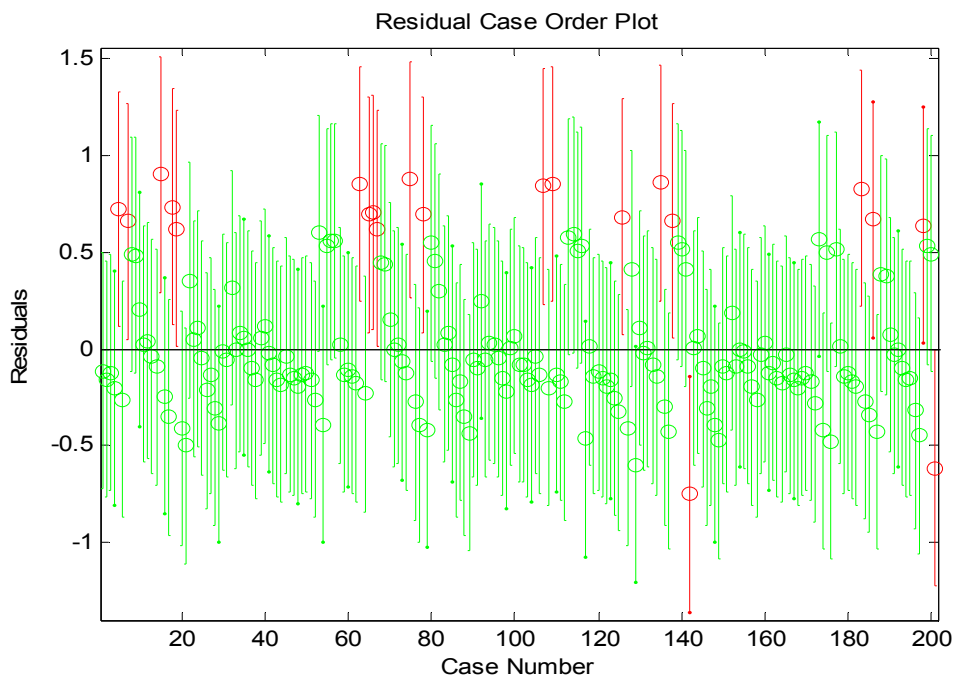


**Figure 4.5** Residual values (2001 to 2200) for RS of  $P_D$  with full factorial experiments.

Although the model obtained with full factorial design gives worse error values than D-optimal model, expected factor dependencies can be observed with this model. Expected correlation of target mean and seed center is clearly detected from Figure 4.3. Maximum probability of detection is obtained when the seed center parameter is tuned around target mean and remaining parameters are held constant.

Also it is observed that increasing target upper bound intensity value and grow threshold decreases probability of detection when remaining parameters are held constant. This is because of the increasing probability of overflowing the target region. Small values of these parameters guarantees staying inside the target region although this produces worse segmentation accuracy.

Increasing target contrast increases detection probability as observed from Figure 4.3 and as expected.

One interesting result of the model is that increasing standard deviation of the target increases probability of detection effectively. This is because of an unconsidered factor of probability of detection. This factor is the target area. Probability of detection increases as standard deviation because standard deviation increases with increasing target area. Standard deviation is nearly directly proportional with target area in used training database. (See Figure 2.8 and Figure 2.14)

Both of the models obtained for  $P_D$  used target dependent metrics. These metrics needs groundtruth of the target. The approach is to estimate the groundtruth from the archived frames starting by tracking order of an operator (operator is pointing out the groundtruth target). The estimated groundtruth can then be used to extract target dependent image metrics. In cases where this information cannot be obtained regional image metrics (Section 3.3) can be used to increase the probability of detection. Although various general-purpose regional metrics can be found the best choice for regional metrics must rely on the target definition of the ATD system. For our system the best choice of regional metrics is classification features. Then

false alarm rate can be used (i.e increasing false alarm rate) to increase the  $P_D$  because false alarms are objects that cannot be distinguished from targets.

### 4.3.2 Segmentation Accuracy (SA)

Evaluation of SA for the proposed ATD algorithm is explained in Section 2.4.6. Regarding the algorithm, three target dependent image metrics and three ATD algorithm parameters are selected as factors of the SA response surface. Selected parameters, image metrics and experimental design (full factorial) are same with the ones used for full factorial design of  $P_D$ . Only response variable is changed as segmentation accuracy.

Then, for SA obtained experiment points and responses are fitted on the model with “rstool” function of MATLAB software. (Figure 4.6)

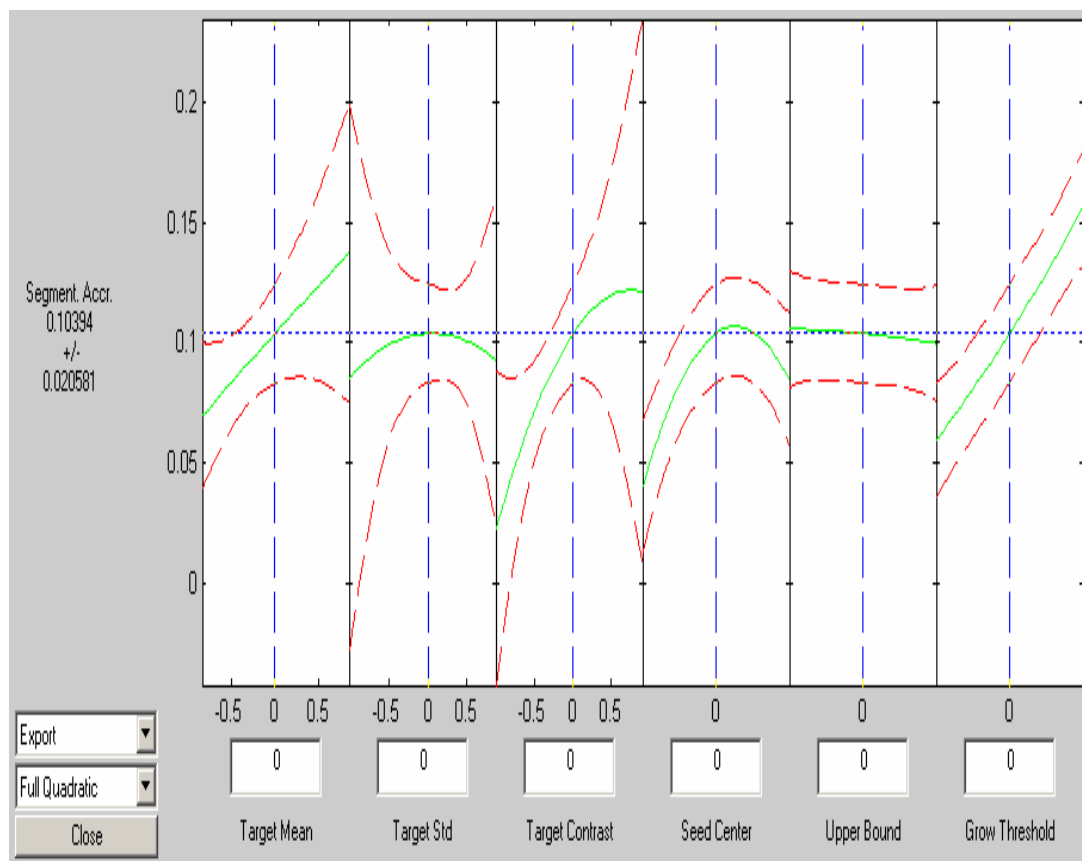


**Figure 4.6** Response surface for SA with full factorial experiments.

RMSE and  $R^2$  values for this model are given below:

RMSE of this model is: 0.1173

Coefficient of multiple determination ( $R^2$ ) = 0.1519

Residual values from (1 to 200) and (2001 to 2201) together with their confidence intervals for the mean are plotted on Figure 4.7 and Figure 4.8. Residuals that do not include zero (outliers) in their confidence interval are shown in these figures.

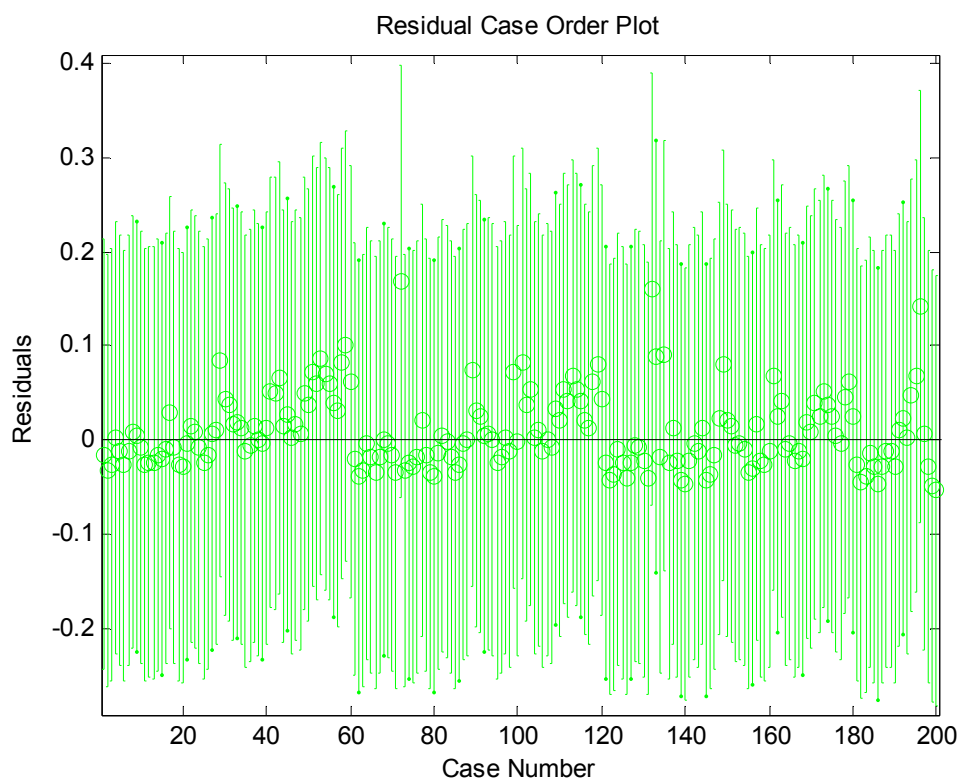


**Figure 4.7** Residual values (1 to 200) for RS of SA with full factorial experiments.

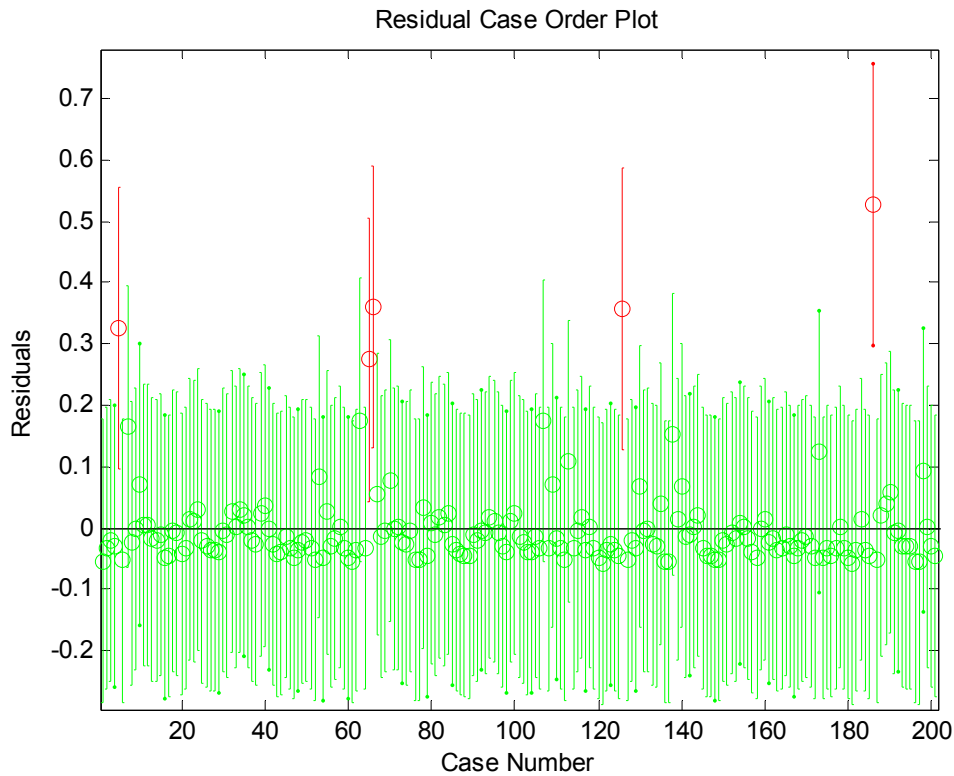


**Figure 4.8** Residual values (2001 to 2200) for RS of SA with full factorial experiments.

Although the error values are high, it is seen that the model makes sense when factor effects are considered. Obtained model for SA is correlated with the model for  $P_D$  because SA value is zero when probability of detection is zero. Then, factors that effect to SA and PD on the same way is observed similarly on SA model (SA increases with Target Contrast as  $P_D$  increases with Target Contrast).

But contradicting factor effects are suppressed or even reversed in SA model. It was seen that increasing Target Std increases  $P_D$ . But increasing Target Std is expected to decrease segmentation accuracy (knowledge from segmentation algorithm). Because of this contradiction it is observed in SA model that, effect of Target Std is suppressed with respect to the effect in  $P_D$ .

This effect is also seen on Grow Contrast. It is observed that increasing Grow Threshold decreases  $P_D$  (Figure 4.3) but it is expected that increasing Grow

Threshold increases SA. This contradiction suppresses and reverses the effect of Grow Threshold observed in model of  $P_D$ .

### **4.3.3 False Alarm Rate (FAR)**

Evaluation of FAR for the proposed ATD algorithm is explained in Section 2.4.6. Four global image metrics and three ATD algorithm parameters are selected as factors of the FAR response surface. Selected parameters are same with the used ones for probability of detection and segmentation accuracy. Global image metrics (Global Entropy, Global Standard Deviation, Global Uniformity, and Occurrence Based Uniformity) are used because the false alarm is mainly dependent on whole image.

Instead of designing a new full factorial design for experiment points, design for  $P_D$  is taken and experiment points are updated with new global image metrics. Then, obtained experiment points and responses are fitted on the model with “rstool” function of MATLAB software. (Figure 4.9)

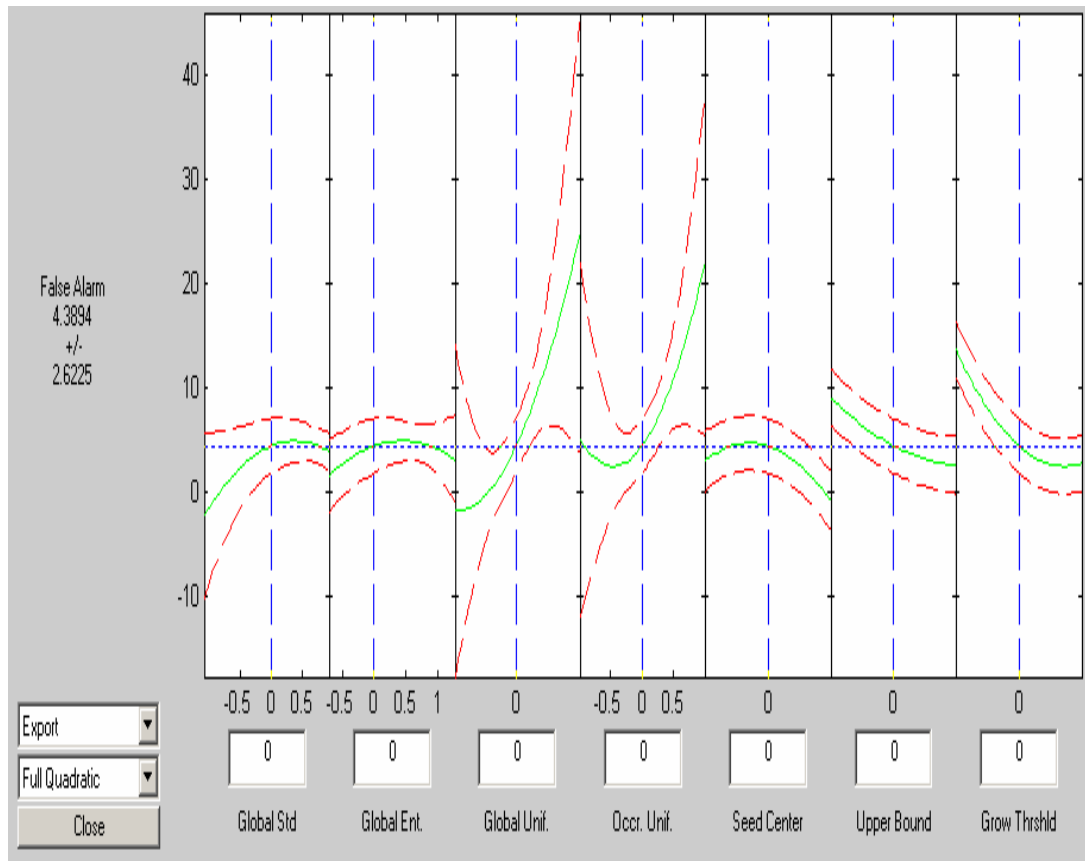


**Figure 4.9** Response surface for FAR with full factorial experiments.

RMSE and  $R^2$  values for this model are given below:

RMSE of this model is: 6.7762

Coefficient of multiple determination ( $R^2$ ) = 0.3750

Residual values together with their confidence intervals for the mean are plotted on Figure 4.10. Residuals that do not include zero (outliers) in their confidence interval are shown in these figures.

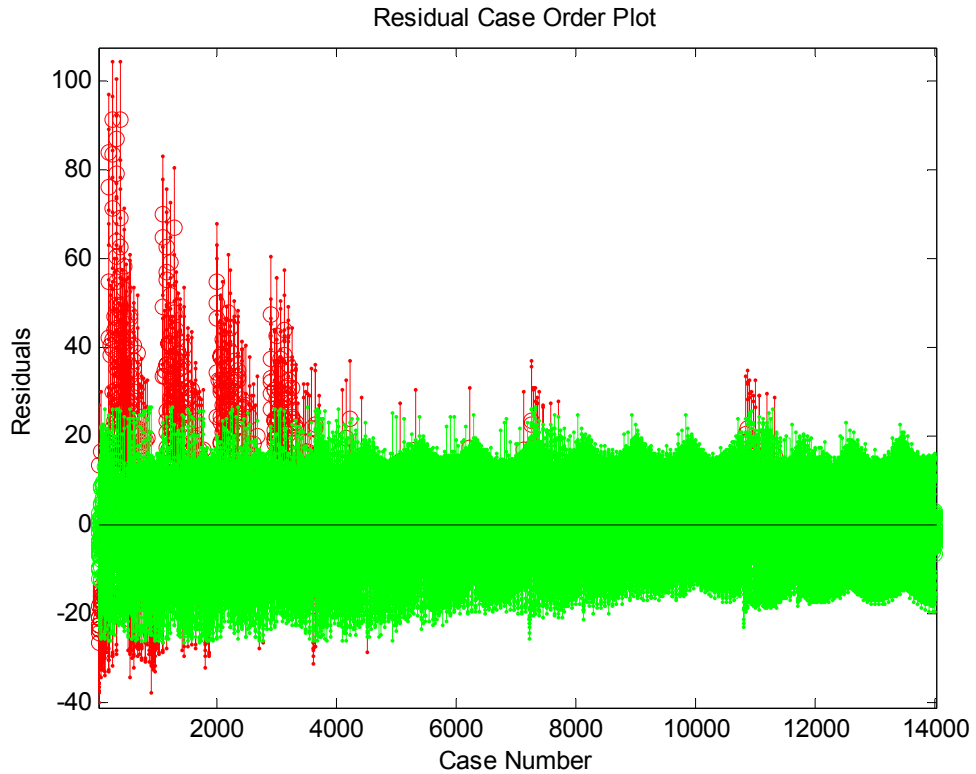


**Figure 4.10** Residual values (1 to 14.000) for RS of FAR with full factorial experiments.

The residuals show contradiction with the assumption of random error. This may be because of the experimental method used or unconsidered unrandomized factors that effect false alarm rate or both. But the model still gives information about the false alarm rate as expected. It is observed that global image metrics that uses local uniformity to characterize the global uniformity are highly correlated with false alarm rate. Also it is observed that false alarm increases with decreasing target upper bound intensity and grow threshold as expected.

## CHAPTER 5

### OPTIMIZATION and TEST RESULTS

#### 5.1 Introduction

Optimization techniques are used to find a set of design parameters  $x = \{x_1, x_2, \dots, x_n\}$  that can in some way be defined as optimal. In a simple case this might be the minimization or maximization of some system characteristic that is dependent on  $x$ . In a more advanced formulation the objective function,  $f(x)$ , to be minimized or maximized, might be subject to constraints in the form of equality constraints, inequality constraints and parameter bounds.

A General Problem (GP) description is stated as,

$$\begin{aligned} &\text{Minimize } F(x) \\ &x \in \mathfrak{R}^n \end{aligned} \tag{5.1}$$

subject to

$$G_i(x) = 0, \quad i = 1, \dots, m_e \tag{5.2}$$

$$G_i(x) \leq 0, \quad i = m_e + 1, \dots, m \tag{5.3}$$

$$x_l \leq x \leq x_u \tag{5.4}$$

where  $x$  is the vector of design parameters ( $x \in \mathfrak{R}^n$ ) with upper and lower bounds ( $x_u, x_l$ ),  $F(x)$  is the objective function that returns a scalar value ( $F(x): \mathfrak{R}^n \rightarrow \mathfrak{R}$ ), and the vector function  $G(x)$  returns the values of the equality and inequality constraints evaluated at  $x$  ( $G(x): \mathfrak{R}^n \rightarrow \mathfrak{R}^m$ ).

An efficient and accurate solution to this problem depends not only on the size of the problem in terms of the number of constraints and design variables but also on characteristics of the objective function and constraints. Objective functions that will be used in this work are performance models obtained in Chapter 4. A wide range spectrum of methods exists for optimizing these models individually subjected to several constraints (i.e. maximizing probability of detection given image metrics of the model by ATD system parameters) [22]. But the general problem definition for ATD systems is different because more than one objective function (performance measures) exists that must be traded off in some way. This problem is known as multiobjective optimization.

In second section of this chapter multiobjective optimization is explained generally and in the third section, applications of multiobjective optimization for the proposed ATD algorithm using performance models are described. Tests and results obtained using these optimization methods on two image sequences are given in the last section of this chapter.

## **5.2 Multiobjective Optimization**

Multiobjective optimization is concerned with the minimization of a vector of objectives  $F(x)$  that can be the subject of a number of constraints or bounds. Because  $F(x)$  is a vector, if any of the components of  $F(x)$  are competing, there is no unique solution to this problem. Instead, the concept of noninferiority must be used to characterize the objectives [22]. A noninferior solution is one in which an improvement in one objective requires a degradation of another. To define this

concept more precisely, consider a feasible region,  $\Omega$ , in the parameter space  $x \in \mathfrak{R}^n$  that satisfies all the constraints.

This allows us to define the corresponding feasible region for the objective function space  $\Lambda$ .

$$\Lambda = \{y \in \mathfrak{R}^m\} \text{ where } y = F(x) \text{ subject to } x \in \Omega$$

The performance vector,  $F(x)$  maps parameter space into objective function as is represented for a two-dimensional case in Figure 5.1.

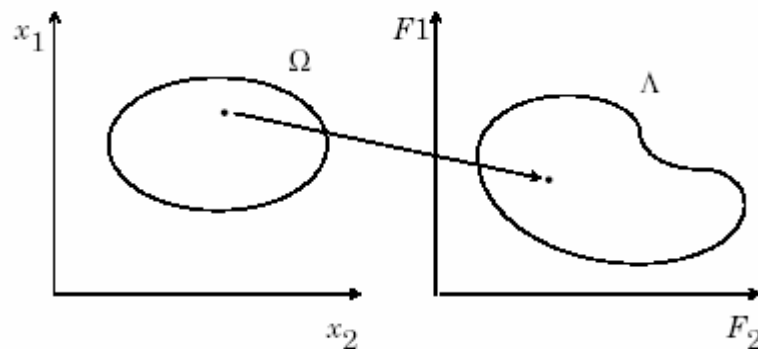


**Figure 5.1** Mapping from parameter space into objective function space.

A noninferior solution point can now be defined as a point  $x^* \in \Omega$  that for some neighborhood of  $x^*$  there does not exist a  $\Delta x$  such that  $(x^* + \Delta x) \in \Omega$  and

$$F_i(x^* + \Delta x) \leq F_i(x^*) \quad i=1, \dots, m \quad (5.5)$$

$$F_j(x^* + \Delta x) \leq F_j(x^*) \text{ for some } j \quad (5.6)$$

In the two-dimensional representation of Figure 5.2, the set of noninferior solutions lies on the curve between C and D. Points A and B represent specific noninferior points.

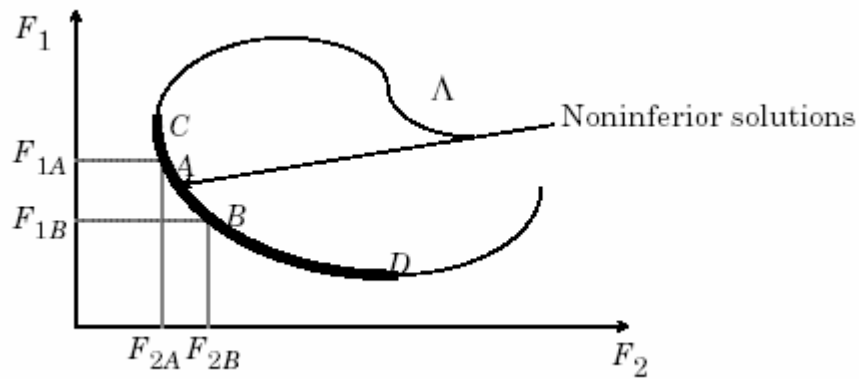


**Figure 5.2** Set of Noninferior Solutions

A and B are clearly noninferior solution points because an improvement in one objective,  $F_1$ , requires a degradation in the other objective,  $F_2$ . Since any point in  $\Omega$  that is not a noninferior point represents a point in which improvement can be attained in all the objectives, it is clear that such a point is of no value. Multiobjective optimization is, therefore, concerned with the generation and selection of noninferior solution points. Two simple problem formulations for handling noninferior solution points is given below.

### **Weighted Sum Strategy**

The weighted sum strategy converts the multiobjective problem of minimizing the vector  $F(x)$  into a scalar problem by constructing a weighted sum of all the objectives.

$$\begin{aligned} &\text{minimize } f(x) = \sum_{i=1}^m w_i F_i(x)^2 && (5.7) \\ &x \in \Omega \end{aligned}$$

The problem can then be optimized using a standard unconstrained optimization algorithm. The problem here is in attaching weighting coefficients to each of the objectives. The weighting coefficients do not necessarily correspond directly to the relative importance of the objectives or allow tradeoffs between the objectives to be

expressed. Further, the noninferior solution boundary can be nonconcurrent, so that certain solutions are not accessible.

### **$\varepsilon$ -Constraint Method**

A procedure that overcomes some of the convexity problems of the weighted sum technique is the  $\varepsilon$ -constraint method. This involves minimizing a primary objective,  $F_p(x)$ , and expressing the other objectives in the form of inequality constraints,

$$\begin{aligned} &\text{Minimize } F_p(x) \\ &x \in \Omega \end{aligned} \tag{5.8}$$

subject to

$$F_i(x) \leq \varepsilon_i \quad i=1 \dots m \quad i \neq p \tag{5.9}$$

This approach is able to identify a number of noninferior solutions on a nonconvex boundary that are not obtainable using the weighted sum technique. A problem with this method is, however, a suitable selection of  $\varepsilon$  to ensure a feasible solution. A further disadvantage of this approach is that the use of hard constraints is rarely adequate for expressing true design objectives.

### **5.3 ATD Optimization**

The common objective of all ATD systems is to increase probability of detection and segmentation accuracy while decreasing false alarm rate. A generally experienced problem is that these performance measures contradict with each other (i.e High probability of detection requires high false alarm rate). In this case there must be a trade off for these performance measures. Generally these trade offs are determined specifically for the system (i.e system capacity determines maximum

false alarm rate or weapon specifications determine the segmentation accuracy) and may appear in the form of constraints such as

$$\begin{aligned} & \text{maximize } P_D(x) \\ & x \in \Omega \end{aligned} \tag{5.10}$$

subject to

$$FAR(x) \leq \varepsilon_{FAR} \text{ or } SA(x) \geq \varepsilon_{SA} \tag{5.11}$$

Then the problem of optimization turns into the  $\varepsilon$ -constraint method for multiobjective optimization. The Optimization Toolbox of MATLAB software provides the function “fmincon” that can be used for this purpose. This function finds a minimum of a constrained nonlinear multivariable function using sequential quadratic programming:

$$\begin{aligned} & \text{minimize } F(x) \\ & x \end{aligned} \tag{5.12}$$

subject to

$$C(x) \leq 0 \tag{5.13}$$

$$Ceq(x) = 0 \tag{5.14}$$

$$A.x \leq b \tag{5.15}$$

$$A_{eq}.x = b_{eq} \tag{5.16}$$

$$lb \leq x \leq ub \tag{5.17}$$

where  $x$ ,  $b$ ,  $b_{eq}$ ,  $lb$  and  $ub$  are vectors,  $A$  and  $A_{eq}$  are matrices,  $C(x)$  and  $Ceq(x)$  are functions that return vectors, and  $F(x)$  is a function that returns a scalar.  $F(x)$ ,  $C(x)$ , and  $Ceq(x)$  can be nonlinear functions.

Then two optimization problems for the proposed ATD algorithm are defined and solved using this MATLAB function.

$$1. \begin{aligned} &\text{maximize } P_D(x) \\ &x \in \Omega \end{aligned} \tag{5.18}$$

subject to

$$FAR(x) \leq \varepsilon_{FAR} \tag{5.19}$$

$$2. \begin{aligned} &\text{maximize } P_D(x) \\ &x \in \Omega \end{aligned} \tag{5.20}$$

subject to

$$-SA(x) \leq \varepsilon_{SA} \tag{5.21}$$

A typical function call to this function is follows:

$$X=fmin(@objectfun,[init],[],[],[],[lb],[ub],@confun,options,[metrics]) \tag{5.22}$$

With this call the function minimizes the “objectfun” regarding the constraints written in “confun” starting with “init” vector position and upper and lower bound of “lb” and “ub”. Vector of “metrics” passes the image metrics for the constraint evaluation.

#### 5.4 Test Results

Both of the solutions are tested on two image sequences (Test Sequence\_1, Test Sequence\_2) including 60 and 50 frames respectively. Two sample images from these test sequences are shown in Figure 5.3 and Figure 5.4. Also target dependent metrics for these image sequences are given in Figure 5.5 and Figure 5.6. Images are obtained by a thermal camera and test sequences are formed by 1/20 downsampling from 25 frame/sec. camera output.



**Figure 5.3** Sample frame from Test Sequence\_1.



**Figure 5.4** Sample frame from Test Sequence\_2.

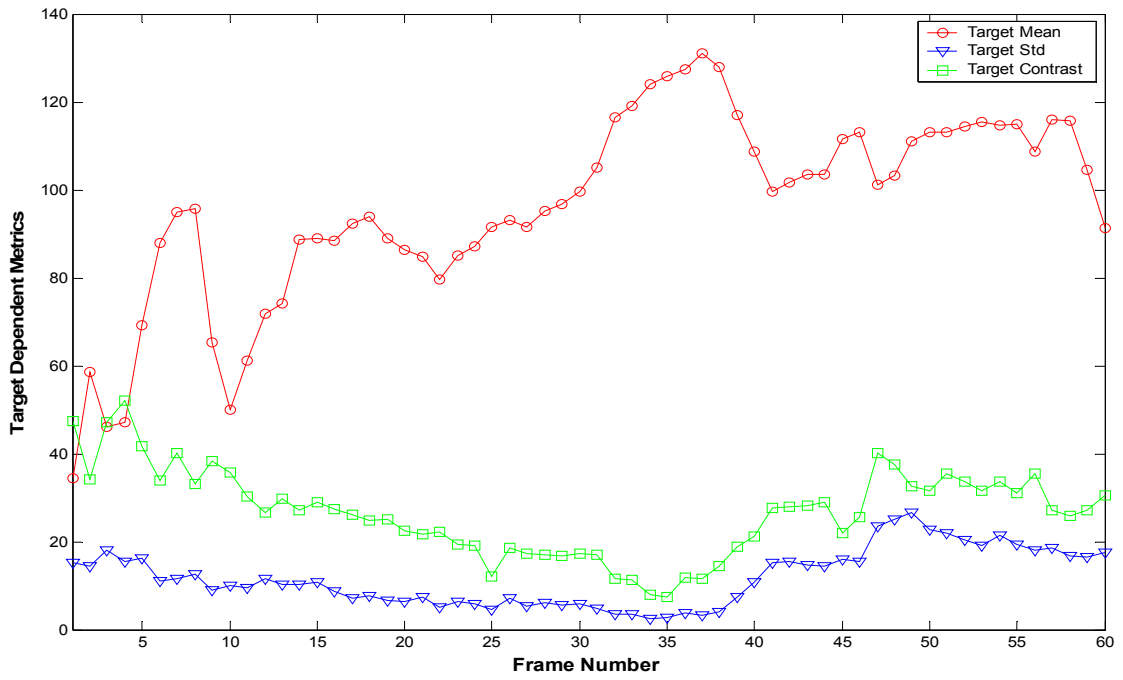


Figure 5.5 Target dependent metrics of Test Sequence\_1.

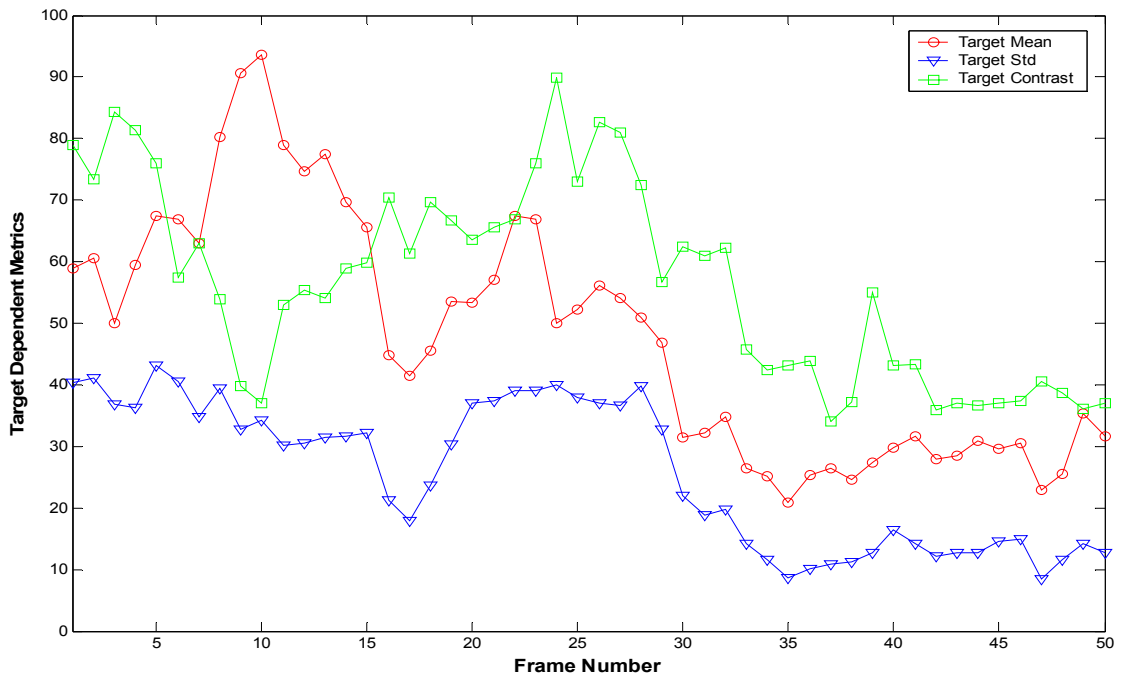


Figure 5.6 Target dependent metrics of Test Sequence\_2.

The pseudo code for the conducted tests is as follows:

```
Read Target Dependent Image Metrics from file for Frame Number 1,  
For Frame Number:2 to 60/50 (For Test Sequence 1/2)  
  Begin  
    Compute Global Image Metrics from frame (For problem 1),  
    Find optimum parameters, given image metrics,  
    Run ATD algorithm,  
    If  $P_D=1$   
      Compute Target Dependent Image Metrics,  
    Else  
      Read Target Dependent Image Metrics from file,  
  End
```

Results are given under two problem definitions made in Section 5.3.

### **1. Maximizing $P_D$ with Constraint on FAR**

Performance models for  $P_D$  and FAR are used for this purpose. Model for  $P_D$  is taken as objective function and model for FAR is used to limit FAR value to a maximum of 10. Probability of detection and false alarm rates are given in Figure 5.7, Figure 5.8 and Figure 5.9.

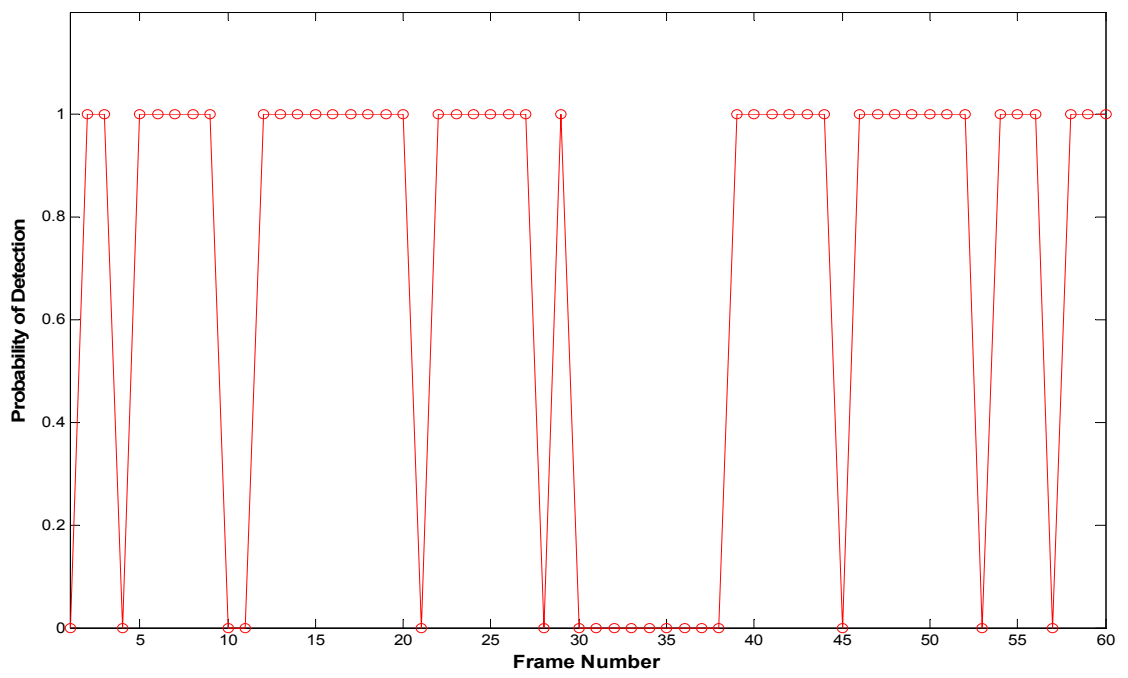


**Figure 5.7** Probability of Detection (Constraint on FAR) for Test Sequence\_1

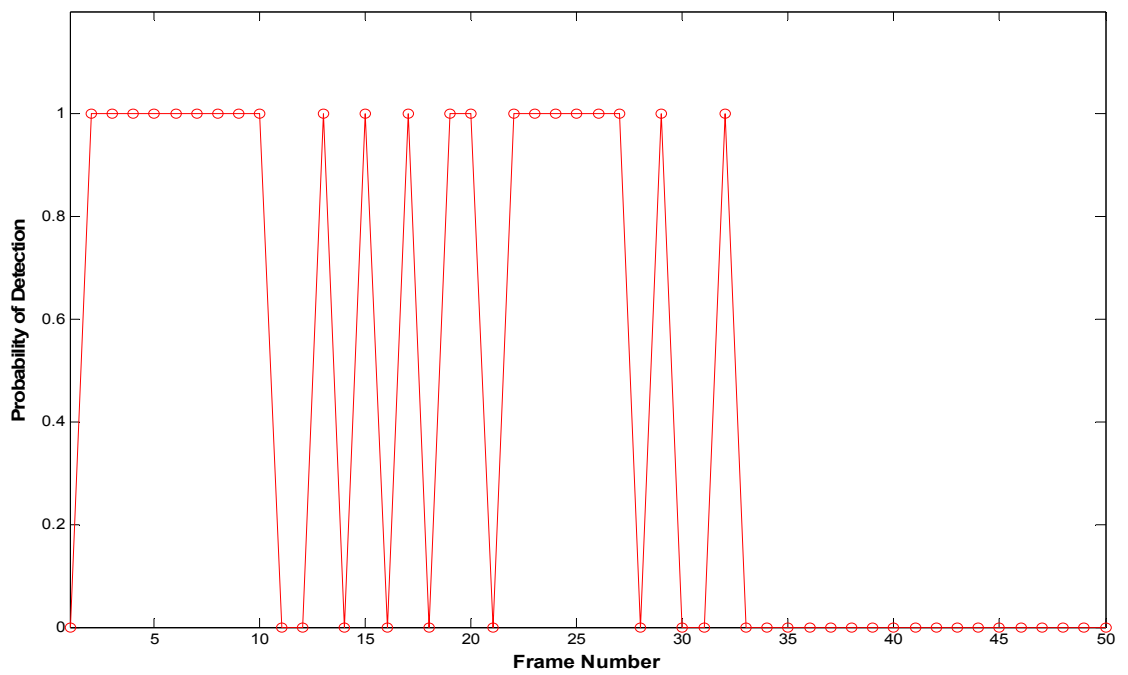


**Figure 5.8** Probability of Detection (Constraint on FAR) for Test Sequence\_2

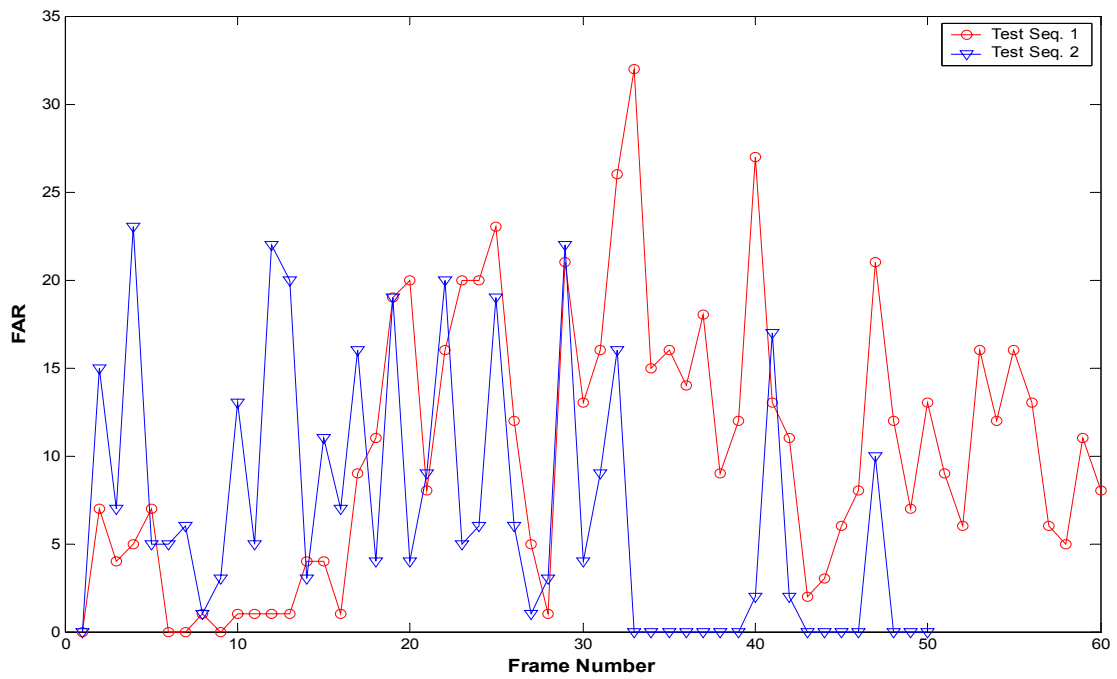


**Figure 5.9** FAR for Test Sequence\_1/2

## 2. Maximizing $P_D$ with Constraint on SA

Performance models for  $P_D$  and SA are used for this purpose. Model for  $P_D$  is taken as objective function and model for SA is used to limit FAR value to a minimum value of 0.1. Probability of detection and false alarm rates are given in Figure 5.10, Figure 5.11 and Figure 5.12.

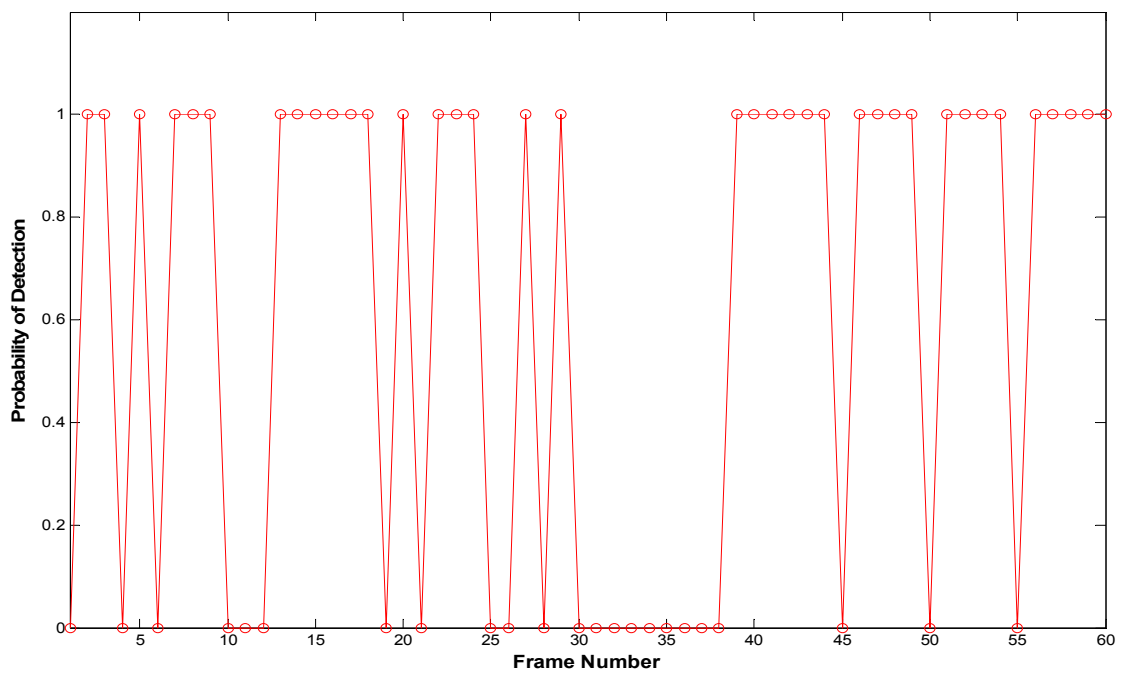


**Figure 5.10** Probability of Detection (Constraint on SA) for Test Sequence\_1

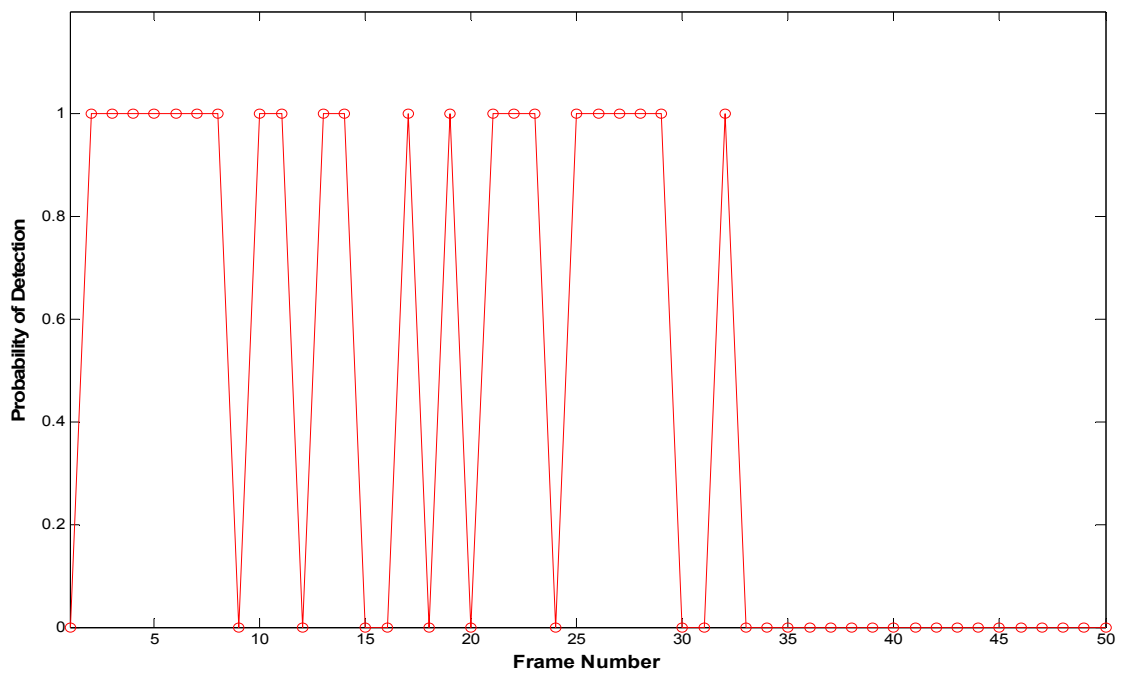


**Figure 5.11** Probability of Detection (Constraint on SA) for Test Sequence\_2

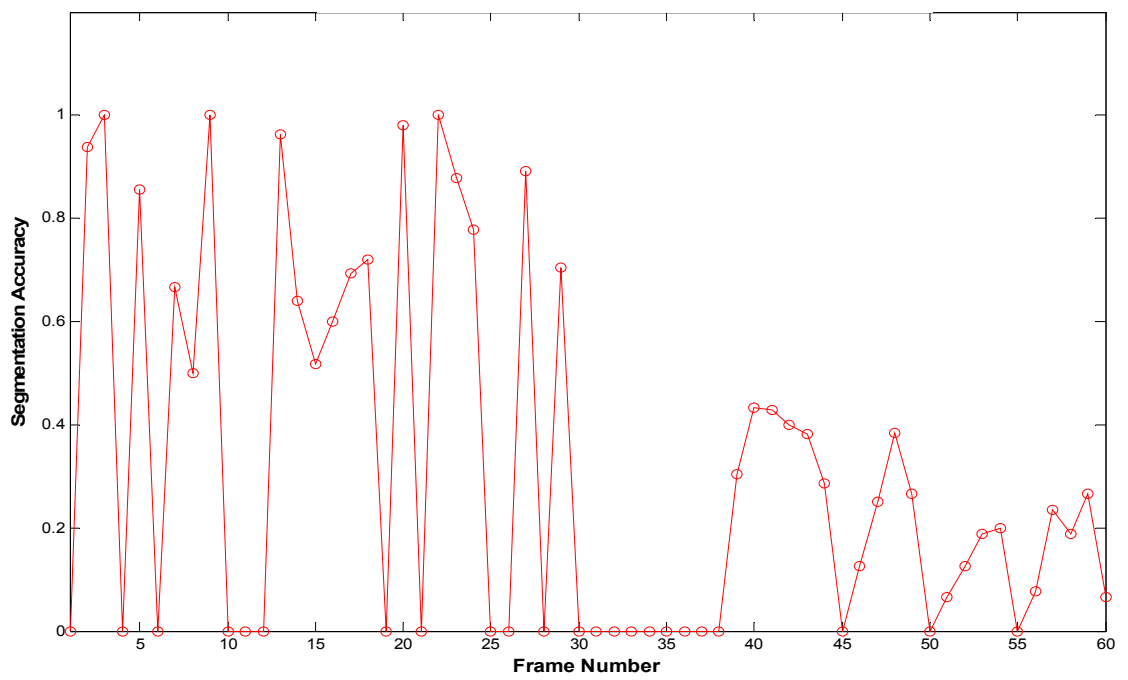


**Figure 5.12** Segmentation Accuracy for Test Sequence\_1

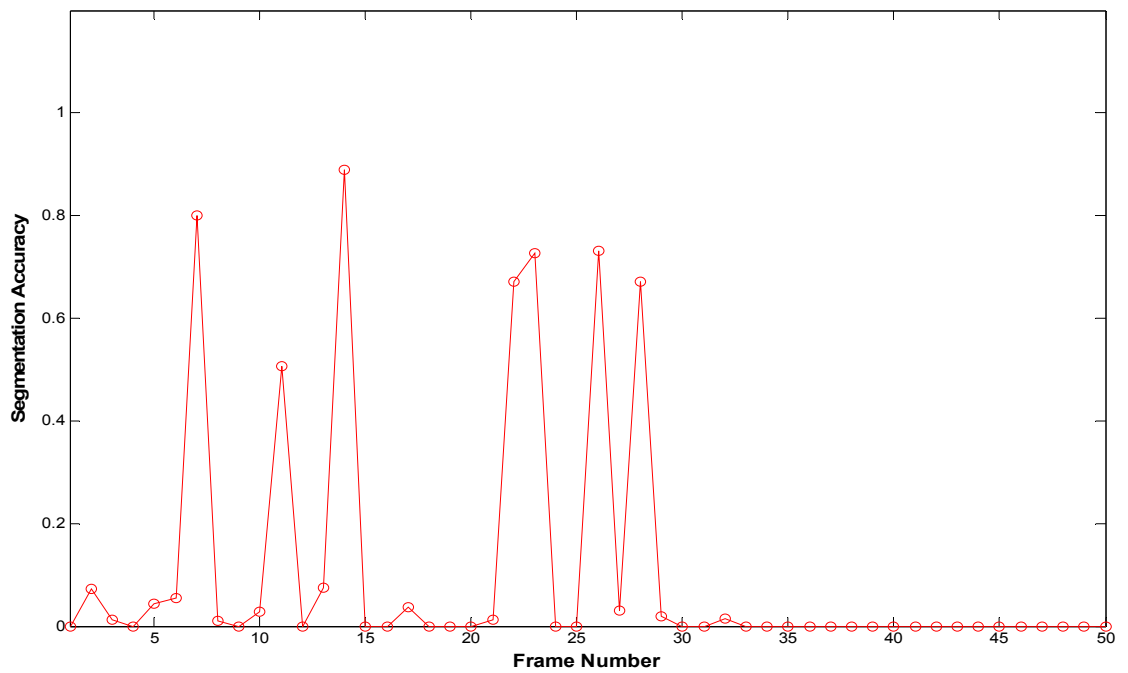


**Figure 5.13** Segmentation Accuracy for Test Sequence\_2

The most important observation for both optimization problems and for both test sequences about probability of detection is that detection fails when target standard deviation and target to background contrast are both low (Figure 5.5 and Figure 5.6). These results show that the model for  $P_D$  is not adequate for this combination of target standard deviation and target to background contrast values.

Results about false alarm rate and segmentation accuracy show that maximum FAR and minimum SA can not be achieved for some frames on test sequences although the optimization process achieves this for the model. This result is not unexpected because of the inaccuracy of the used models for FAR and SA.

Figures 5.14 and 5.15 show PD obtained for optimization problem 1 with non-optimal -0.1 below optimal system parameters- system parameters. Decrease in performance is easily observed with respect to figures 5.7 and 5.8.

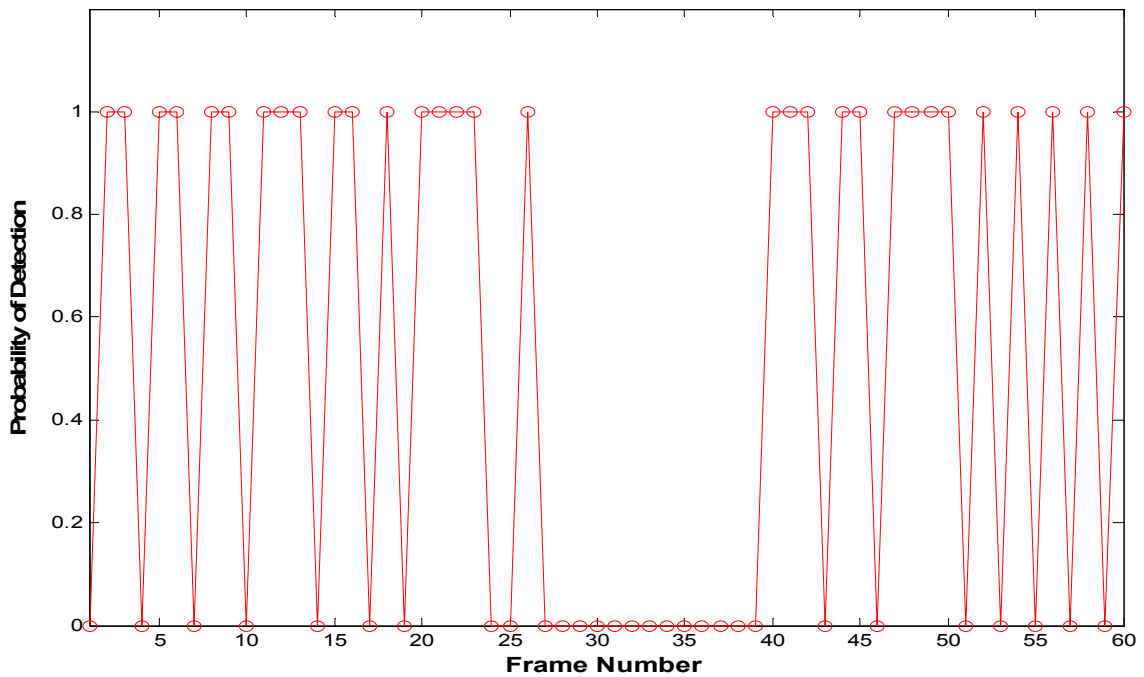


**Figure 5.14** Non-Optimal Probability of Detection (Constraint on FAR) for Test Sequence\_1

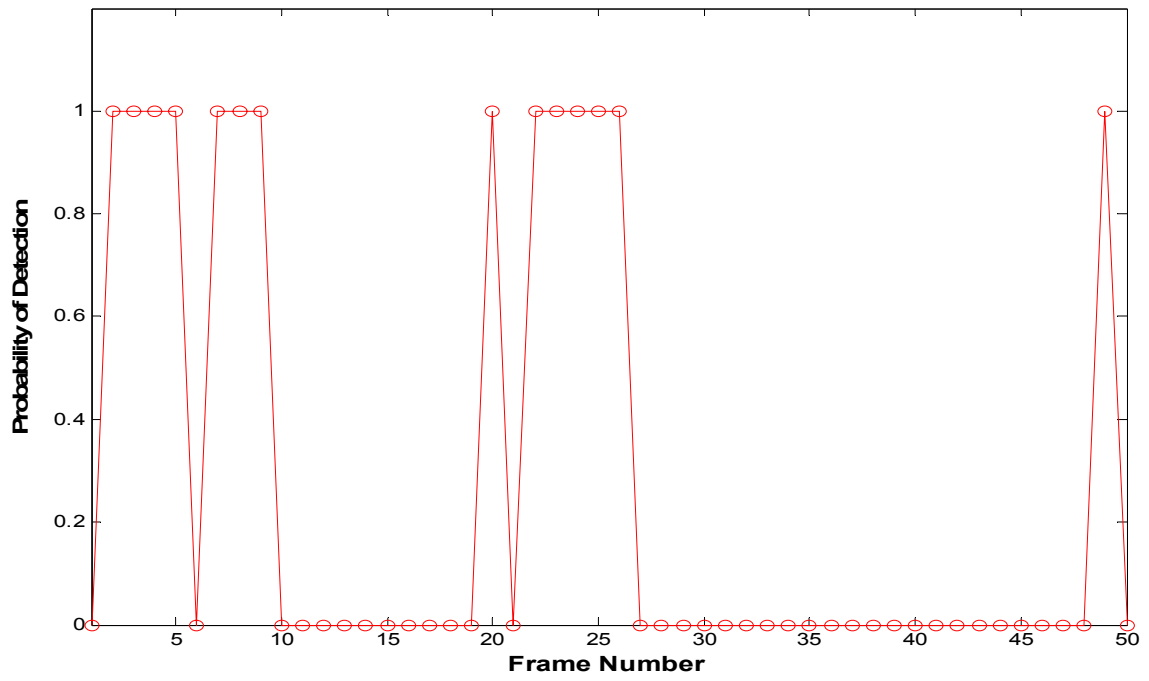


**Figure 5.15** Non-Optimal Probability of Detection (Constraint on FAR) for Test Sequence\_2

## **CHAPTER 6**

### **CONCLUSION and FUTURE WORK**

#### **6.1 Summary and Conclusion**

In this thesis we have attempted to model performance metrics of an ATD system with image metrics and ATD system parameters. The main purpose to form these models is to optimize the performance of the system by changing system parameters using measured image metrics based on these models.

A simple ATD system is proposed. Three performance measures namely, probability of detection, segmentation accuracy and false alarm rate are used as system evaluation methods. In order to characterize image, global, regional and target dependent metrics are used. Image metrics and ATD system parameters are selected for each of the performance measure and experiments are designed to determine experimental points (image metric and parameter value combinations). Then experiments are conducted for these experimental points and results are fitted on quadratic multivariate linear regression models using MATLAB. Consequently models are obtained for each of the performance measures.

Obtained models are used to solve an optimization problem of ATD systems. The problem was to maximize probability of detection with limits on false alarm rate or segmentation accuracy. Functions of MATLAB software is used to apply the solution to these problems and solutions are tested on two sequences. It is observed that the model regions where there exist experimental insufficiencies do not predict optimum (or better) system parameters. Due to this, optimization with

respect to these models improves the ATD system performance when the incoming image metrics are on the “reliable” region of the models.

One experimental insufficiency is due to the restricted training database which does not provide all experimental points. This reduces the prediction capability of the model around these points. Another insufficiency is selection of ATD system parameters. Adaptable parameter about seed points is only the center of the seeds. This selection can not deal with targets with low standard deviation and low target to background contrast because it uses seeds within fixed range of ten for all seed center values (pixels take intensity values from 0 to 255). In other words there is no “good” parameter value to this case in the model. Nevertheless optimization based on these models improved the system performance for reliable regions of the models.

## **6.2 Future Work**

This methodology to develop performance models can also be used to analyze the effects of image characteristics and parameters to the performance of an ATD system. This seems a simple task for this work but a typical ATD system has 10s of parameters (most of them are constant) and effects of these parameters are not easily determined by simply considering system knowledge especially when there is interaction between parameters. Not for making these parameters adaptive, but for finding optimum values this method can be used.

The critical part of this methodology is the performance models. Models with better prediction capability will result in better adaptation of system parameters to improve system performance. Prediction capability is highly related with characterizing image with metrics. Finding or developing metrics that better characterize image for the ATD system may be a future work that improves the usefulness of the methodology.

In this thesis only ATD system parameters are used to model and optimize performance measures. In most of the commercial ATD systems more than one algorithm is provided that each works better in some scenario. The decision for changing these alternative algorithms with respect to the scenario is taken by the operator of the ATD system. An application of this methodology can be to take this decision automatically and reliably with image metrics.

## REFERENCES

- [1] J. A. Ratches, C. P. Walters, R. G. Buser, and B. D. Guenther, "Aided and Automatic Target Detection Based Upon Sensory Inputs From Image Forming Systems," IEEE Transactions On Pattern Analysis And Machine Intelligence, Vol. 19, No. 9, September 1997
- [2] C. Zhou, G. Zhang, J. Peng, Institute of Image Detection and Artificial Intelligence, Huazhong University of Science and Technology, Hubei, Wuhan P.R. Chine, "Performance Modeling Based Adaptive Target Tracking in Multiscenario Environment," Proceedings of SPIE Vol. 2756, 1996
- [3] H. Nasr, M. Bazakos, F. Sadjadi, and H. Amehdi, Honeywell Inc. Systems and Research Center, "Knowledge and model Based ATD Algorithms Adaptation," SPIE Institute Series Vol. IS, 1990
- [4] B. Bhanu, University of Utah, "Automatic Target Detection: State of the Art Survey," IEEE Transactions on Aerospace and Electronic Systems, Vol. Aes-22, No.4 July 1986
- [5] F. Sadjadi, Honeywell Inc. Systems and Research Center, "Automatic Object Detection: Critical Issues and Current Approaches," Proceedings of SPIE Vol. 1471, 1991
- [6] W. M. Brown, C. W. Swonger, Environmental Research Institute of Michigan, "A Prospectus for Automatic Target Detection, IEEE Transactions on Aerospace and Electronic Systems," Vol. 25, No.3 May 1989

- [7] R. Adams, L. Bischof, "Seeded Region Growing, IEEE Transactions On Pattern Analysis And Machine Intelligence," Vol. 16, No. 6, June 1994
- [8] B. Sankur, M. Sezgin, "Image Thresholding Techniques: A Survey Over Categories," submitted to Pattern Detection, 2001
- [9] R. A. Peters, R. N. Strickland, "Image Complexity Metrics for Target Recognizers," Automatic Target Recognizer System and Technology Conference 1990
- [10] B. Bhanu, "Automatic Target Detection: State of the Art Survey," IEEE Trans. Aero. and Elec. Sys., vol. AES-22, No. 4, pp. 364-379, 1986
- [11] M. D. Levine, and M. N. Nazif, "Dynamic Measurement of Computer Generated Image Segmentations," IEEE Trans. Pattern Anal. Machine Intell., vol. PAMI-7, No.2 pp. 38-48, 1985
- [12] S. R. Rotman, G. Tidhar, M. L. Kowalczyk, "Clutter Metrics for Target Detection Systems," IEEE Transactions on Aerospace and Electronic Systems, Vol. 30, No. 1, January 1994
- [13] T. Meitzler, G. Gerhart, H. Singh, "A Relative Clutter Metric," IEEE Transactions on Aerospace and Electronic Systems, Vol. 34, No. 3 July 1998
- [14] K. R. Namuduri, K. Bouyoucef, L. M. Kaplan, "Image Metrics for Clutter Characterization," IEEE, 2000
- [15] J. Beard, L. Clark, and V. Velten, "Characterization of ATD performance in relation to image measurements," ATDWG report, AFWAL/AARF, Wright Patterson AFB, OH, 45433, Mar., 1985
- [16] Statistical Toolbox For Use with MATLAB, User's Guide by Matworks Inc. 2002

- [17] Douglas C. Montgomery, Design and Analysis of Experiments John Wiley&Sons Inc. 2001
- [18] Fundamentals of Automatic Target Recognition, Short Courses by Hatem Nasr, International Society for Optical Engineering, 2000
- [19] Dan E. Dungeon, W. Eric L. Grimson, and Robert Tenney, Issues in SAR Model-Based Target Recognition, SPIE Vol. 2484
- [20] M. W. Roth, Survey of Neural Network Technology for Automatic Target Recognition, IEEE Trans. Neural Networks, vol. 1, no.1, Mar. 1990
- [21] M. Soysal, Combining Image Features for Semantic Descriptions, September 2003.
- [22] Optimization Toolbox For Use with MATLAB, User's Guide by Matworks Inc. 2002

## APPENDIX A

### MODEL INFORMATION

**Table A.1** Factor Maximum and Minimum Values for D-Optimal Experimental Design of  $P_D$

	<b>Target Mean</b>	<b>Target Std</b>	<b>Target Contrast</b>	<b>Seed Center</b>	<b>Seed Range</b>	<b>Grow Threshold</b>
<b>Min.</b>	70 (-1)	10 (-1)	10 (-1)	70 (-1)	3 (-1)	3 (-1)
<b>Center</b>	120 (0)	30 (0)	40 (0)	120 (0)	9 (0)	9 (0)
<b>Max.</b>	170 (1)	50 (1)	70 (1)	170 (1)	15 (1)	15 (1)

**Table A.2** Ideal D-Optimal Experimental Design for  $P_D$

<b>Target Mean</b>	<b>Target Std</b>	<b>Target Contrast</b>	<b>Seed Center</b>	<b>Seed Range</b>	<b>Grow Threshold</b>
-1	0	1	0	1	-1
1	1	1	1	-1	1
-1	1	1	1	1	1
1	1	-1	1	1	1
0	-1	1	1	-1	-1
1	-1	1	-1	1	-1
-1	-1	1	1	-1	1
-1	-1	1	-1	-1	1
-1	-1	-1	-1	1	1
-1	-1	-1	1	1	1
1	1	1	1	1	-1
1	-1	1	-1	-1	1
-1	1	1	-1	-1	-1
-1	1	-1	-1	-1	1
-1	-1	1	-1	1	1
1	1	1	-1	1	1
-1	-1	1	1	1	-1
1	1	-1	-1	-1	-1
1	-1	-1	-1	-1	1

1	-1	1	1	1	1
1	1	0	-1	-1	0
-1	1	-1	-1	1	-1
1	0	-1	-1	1	1
1	-1	-1	1	1	-1
-1	-1	-1	-1	-1	-1
1	1	1	1	-1	-1
-1	1	1	-1	1	-1
1	-1	-1	0	-1	-1
-1	0	0	1	-1	0
-1	1	1	1	0	-1
-1	-1	0	0	-1	-1
1	-1	-1	-1	1	0
1	1	-1	1	-1	1
1	-1	1	1	0	0
1	1	1	0	1	0
1	1	0	1	1	-1
-1	1	0	1	0	1
1	-1	0	1	-1	1
0	1	-1	1	-1	-1
1	1	1	-1	0	1
-1	1	0	-1	1	1
-1	1	-1	1	1	0
-1	1	-1	1	-1	-1
1	-1	-1	1	-1	0
1	1	-1	-1	1	-1
1	0	-1	1	0	-1
-1	0	-1	-1	0	-1
1	-1	1	-1	-1	-1
-1	-1	-1	1	-1	1
-1	-1	1	-1	0	0
1	0	1	0	-1	-1
-1	1	-1	-1	-1	1
-1	1	1	0	-1	1
-1	-1	-1	1	1	-1
0	1	-1	0	1	0
0	0	1	1	1	1
0	-1	-1	0	0	1
1	-1	0	0	1	1
0	0	1	-1	-1	0
0	-1	0	-1	1	-1
-1	0	1	0	1	-1
1	1	1	1	-1	1
-1	1	1	1	1	1
1	1	-1	1	1	1

0	-1	1	1	-1	-1
1	-1	1	-1	1	-1
-1	-1	1	1	-1	1
-1	-1	1	-1	-1	1
-1	-1	-1	-1	1	1
-1	-1	-1	1	1	1

**Table A.3** Modified D-Optimal Experimental Design and Response Values for  $P_D$

Target Mean	Target Std	Target Contrast	Seed Center	Seed Range	Grow Threshold	$P_D$
-0.9169	0.3731	1.3053	0	1	-1	1
0.3124	0.9230	0.7083	1	-1	1	1
-0.9249	0.7622	1.4500	1	1	1	0
0.5305	-0.3581	-0.8129	1	1	1	0
-0.0133	0.1437	0.3306	1	-1	-1	0
1.0820	-0.8834	-0.6359	-1	1	-1	0
-1.0100	-1.1087	-0.1302	1	-1	1	0
-1.0100	-1.1087	-0.1302	-1	-1	1	0
-0.9400	-0.8945	-0.7563	-1	1	1	0
-0.9400	-0.8945	-0.7563	1	1	1	0
0.2614	2.0314	1.7657	1	1	-1	1
1.0820	-0.8834	-0.6359	-1	-1	1	0
-0.9249	0.7622	1.4500	-1	-1	-1	1
-1.0350	0.2259	-0.9712	-1	-1	1	0
-1.0100	-1.1087	-0.1302	-1	1	1	0
0.2614	2.0314	1.7657	-1	1	1	1
-1.0100	-1.1087	-0.1302	1	1	-1	0
0.5305	-0.3581	-0.8129	-1	-1	-1	0
1.3233	-1.2665	-0.7952	-1	-1	1	0
1.0820	-0.8834	-0.6359	1	1	1	0
0.8544	-0.0389	0.0467	-1	-1	0	0
-1.0350	0.2259	-0.9712	-1	1	-1	0
1.2022	-0.9124	-0.9987	-1	1	1	0
1.3233	-1.2665	-0.7952	1	1	-1	0
-0.9400	-0.8945	-0.7563	-1	-1	-1	0
0.2614	2.0314	1.7657	1	-1	-1	1
-0.9249	0.7622	1.4500	-1	1	-1	1
1.3233	-1.2665	-0.7952	0	-1	-1	0
-0.9460	0.0716	0.1351	1	-1	0	0
-0.9249	0.7622	1.4500	1	0	-1	0
-0.9067	-0.5814	0.0143	0	-1	-1	0
1.3233	-1.2665	-0.7952	-1	1	0	0
0.5305	-0.3581	-0.8129	1	-1	1	0
1.0820	-0.8834	-0.6359	1	0	0	0
0.2614	2.0314	1.7657	0	1	0	1

0.8544	-0.0389	0.0467	1	1	-1	1
-1.0919	0.0582	-0.4935	1	0	1	0
1.0501	-0.5001	-0.3622	1	-1	1	1
-0.0133	0.1437	0.3306	1	-1	-1	0
0.2614	2.0314	1.7657	-1	0	1	1
-1.0919	0.0582	-0.4935	-1	1	1	0
-1.0350	0.2259	-0.9712	1	1	0	0
-1.0350	0.2259	-0.9712	1	-1	-1	0
1.3233	-1.2665	-0.7952	1	-1	0	0
0.5305	-0.3581	-0.8129	-1	1	-1	0
1.1500	-0.9898	-1.0227	1	0	-1	0
-1.0645	-0.0536	-1.1285	-1	0	-1	1
1.0820	-0.8834	-0.6359	-1	-1	-1	0
-0.9400	-0.8945	-0.7563	1	-1	1	0
-1.0100	-1.1087	-0.1302	-1	0	0	0
1.1080	-0.8714	-0.6925	0	-1	-1	0
-1.0350	0.2259	-0.9712	-1	-1	1	0
-0.9249	0.7622	1.4500	0	-1	1	1
-0.9400	-0.8945	-0.7563	1	1	-1	0
-0.1057	-0.2922	-0.5579	0	1	0	0
-0.0675	0.9054	1.0326	1	1	1	0
-0.0680	-1.1750	-0.8748	0	0	1	0
1.0501	-0.5001	-0.3622	0	1	1	0
0.0097	0.7872	0.9025	-1	-1	0	0
-0.0133	-0.7890	-0.2502	-1	1	-1	0
-0.9169	0.3731	1.3053	0	1	-1	1
0.3124	0.9230	0.7083	1	-1	1	1
-0.9249	0.7622	1.4500	1	1	1	0
0.5305	-0.3581	-0.8129	1	1	1	0
-0.0133	0.1437	0.3306	1	-1	-1	0
1.0820	-0.8834	-0.6359	-1	1	-1	0
-1.0100	-1.1087	-0.1302	1	-1	1	0
-1.0100	-1.1087	-0.1302	-1	-1	1	0
-0.9400	-0.8945	-0.7563	-1	1	1	0
-0.9400	-0.8945	-0.7563	1	1	1	0